Aging-associated Increase of GATA4 levels in Articular Cartilage is Linked to Impaired Regenerative Capacity of Chondrocytes and Osteoarthritis

Meagan J. Makarczyk[1,2,#], Yiqian Zhang[1,4,#], Alyssa Aguglia[2], Olivia Bartholomew[2], Sophie Hines[1,2], Kate Li[3], Suyash Sinkar[2], Silvia Liu[5,6], Craig Duvall[7], Hang Lin[1,2,8,*]

[1] Department of Orthopaedic Surgery, University of Pittsburgh School of Medicine, Pittsburgh, PA, USA

[2] Department of Bioengineering, University of Pittsburgh Swanson School of Engineering, Pittsburgh, PA, USA

[3] Department of Biological Sciences, University of Pittsburgh Kenneth P. Dietrich School of Arts & Sciences, Pittsburgh, PA

[4] Xiangya Hospital, Central South University, Changsha, Hunan, China

[5] Department of Pharmacology and Chemical Biology, University of Pittsburgh School of Medicine, Pittsburgh, PA

[6] Organ Pathobiology and Therapeutics Institute, University of Pittsburgh School of Medicine, Pittsburgh, PA

[7] Department of Biomedical Engineering, Vanderbilt University, Nashville, TN, USA

[8] Bethel Family Musculoskeletal Research Center (BMRC), University of Pittsburgh School of Medicine, Pittsburgh, PA, USA

[#] These authors contributed equally

***Correspondence:**

Hang Lin, PhD

350 Technology Drive, Room 417, Pittsburgh, PA, 15219, USA

Phone: 412-624-5503; Fax: 412-624-5544

Email: hal46@pitt.edu

Abstract

Although the causal association between aging and osteoarthritis (OA) has been documented, our understanding of the underlying mechanism remains incomplete. To define the regulatory molecules governing chondrocyte aging, we performed transcriptomic analysis of young and old human chondrocytes from healthy donors. The data predicted that GATA binding protein 4 (GATA4) may play a key role in mediating the difference between young and old chondrocytes. Results from immunostaining and western blot showed significantly higher GATA4 levels in old human or mouse chondrocytes when compared to young cells. Moreover, overexpressing *GATA4* in young chondrocytes remarkably reduced their cartilage-forming capacity *in vitro* and induced the upregulation of proinflammatory cytokines. Conversely, suppressing *GATA4* expression in old chondrocytes, through either siRNA or a small-molecule inhibitor NSC140905, increased the production of aggrecan and collagen type II, and also decreased levels of matrix-degrading enzymes. In OA mice induced by surgical destabilization of the medial meniscus, intraarticular injection of lentiviral vectors carrying mouse *Gata4* resulted in a higher OA severity, synovial inflammation, and pain level when compared to control vectors. Mechanistically, we found that overexpressing GATA4 significantly increased the phosphorylation of SMAD1/5. Our work demonstrates that the aging-associated increase of GATA4 in chondrocytes plays a vital role in OA progression, which may also serve as a target to reduce osteoarthritis in the older population.

Keywords

GATA4, chondrocyte, aging, osteoarthritis, DNA damage

63 **Introduction**

64 Aging is an inevitable phenomenon resulting in limited functionality, loss of structural
65 integrity, and inability to effectively resist injury and disease.[1] Osteoarthritis (OA), the world's
66 most common form of degenerative disease, has been closely associated with the advancement of
67 age.[2] Specifically, OA is estimated to affect 32.5 million Americans, with most cases occurring in
68 adults over the age of 45.[3] In fact, 1 in 3 people over the age of 65 are suffering from OA.[4] There
69 are many contributors linked to the onset and progression of aging, such as organelle dysfunction
70 and telomere shortening,[1] but the molecular mechanism underlying age-related OA has not been
71 fully understood. Prior studies have demonstrated the role of DNA damage on chondrocyte aging
72 due to oxidative stresses, resulting in an aged phenotype.[5,6] Aged cells can also undergo a state
73 similar to permanent cell cycle arrest known as cellular senescence, which leads to a low-grade
74 state of chronic inflammation and contributes to OA onset and progression in aged individuals.[6-8]

75 OA is now considered a whole joint disease, but cartilage degradation still represents the
76 central feature.[3] The physiological role of articular cartilage is to support and protect the bones of
77 diarthrodial joints through absorbing mechanical loads and facilitating frictionless movements.
78 The extracellular matrix (ECM) of the cartilage is composed primarily of collagen type II and
79 glycosaminoglycans (GAGs), and the constant breakdown and rebuilding of ECM components in
80 the cartilage is common in healthy adults.[3,9] Many growth factors contribute to the chondro-
81 supportive environment in the knee joint. Particularly, transforming growth factor-β (TGF-β) plays
82 a key role in maintaining chondrocytes and replenishing ECM loss. However, during OA, TGF-β
83 can induce catabolic processes in chondrocytes, resulting in matrix stiffening, osteophytes, and
84 chondrocyte hypertrophy.[10-12] Furthermore, as we age, the regenerative response of chondrocytes
85 begins to decline.[2] The whole joint nature of OA and the limited regenerative capacity of
86 chondrocytes have contributed to the difficulty in developing disease-modifying osteoarthritis
87 drugs (DMOADs). To date, no DMOADs have reached FDA approval.[3]

88 Currently, OA-associated changes in chondrocytes have been widely examined, which
89 have significantly enhanced our understanding of this disease and promoted the development of
90 potential treatments. However, OA is a combined consequence of different physiological stressors,
91 including aging, injuries, obesity, etc. Therefore, aged chondrocytes in healthy humans without
92 OA do not necessarily exhibit all the features of OA chondrocytes. In this study, to understand key
93 regulators that contribute to an "aged" state in chondrocytes prior to OA onset, we first compared

94 the transcriptome of young and old human chondrocytes isolated from healthy donors without joint
95 diseases and employed unbiased analysis to define the key regulatory molecules that mediate
96 chondrocyte aging. Assessment of the chondrocyte genome demonstrated the upregulation of
97 several factors in aged chondrocytes, and transcription factor GATA binding protein 4 (GATA4)
98 specifically drew our attention since it is associated with DNA damage and cellular senescence.[5,13]
99 Mechanistically, upregulation of GATA4 was shown to increase nuclear factor-κB (NF-κB)
100 pathway activation.[14,15] NF-κB is thought to amplify and potentially propagate cellular senescence
101 during the aging process through the senescence-associated secretory phenotype (SASP), which
102 could contribute to a low-grade state of chronic inflammation.[16] Furthermore, the upregulation of
103 GATA4 in OA chondrocytes was also reported.[17,18] We thus hypothesized that the increased
104 GATA4 level contributes to chondrocyte aging and accelerated OA progression upon injuries. We
105 first tested the hypothesis by increasing or suppressing *GATA4* expression in healthy chondrocytes
106 and examining their cartilage-forming capacity. When *GATA4* was overexpressed, we found that
107 there were alterations to the TGF-β signaling pathway and activation of the NF-κB signaling
108 pathway. We also assessed the role of GATA4 *in vivo* by injecting lentiviral vectors carrying control
109 or mouse *Gata4* genes into the knee joints of OA mice induced by surgically created destabilization
110 of the medial meniscus (DMM). Lastly, a mechanistic study was conducted to explore how GATA4
111 impacts chondrocyte phenotypes and functions.
112

113 **Materials and Methods**

114 **Cell isolation and expansion**

115 Healthy human knee cartilage tissues were harvested from arthritis-free donors through an
116 established protocol with the National Disease Research Interchange (NDRI). This study was
117 approved by the University of Pittsburgh Committee for Oversight of Research and Clinical
118 Training Involving Decedents. Cartilage was diced into ~ 1 mm^3 pieces with a scalpel and
119 incubated with a dissociation medium that was composed of high glucose Dulbecco's Modified
120 Eagle Medium (DMEM, Gibco/Thermo Fisher Scientific, Waltham, MA, United States), 2%
121 Antibiotics-Antimycotics (Life Technologies, Carlsbad, CA, United States), and collagenase type
122 II (1 mg/mL(w/v), Worthington Biochemical Corporation, Lakewood, NJ, United States). 10 mL
123 medium was used for 1g of cartilage, and the treatment lasted for 16 hours in a shaker at 37°C.
124 The mixture was then passed through a 70 μm strainer to collect single chondrocytes. Isolated

125 chondrocytes were seeded in tissue culture flasks at 1×10^4 cells/cm^2 and maintained in growth
126 medium (GM, DMEM containing 10% fetal bovine serum (FBS, Life Technologies) and 1%
127 Antibiotics-Antimycotics). After cells were fully attached to the culture substrate, the medium was
128 changed every three days until cells reached 70-80% confluency. Cells were detached with
129 Trypsin/EDTA (Gibco/ Thermo Fisher Scientific) and passaged.
130
131 **Individual Chondrocyte Monolayer Culture**
132 Chondrocytes isolated from healthy human cartilage were expanded to passage 1 (P1) and plated
133 in tissue culture 6 well plates at P2, treated with GM, and cultured until cells reached 80%
134 confluency. Media changes occurred every two days until cell collection. **Table S1** lists the
135 chondrocyte ages and genders used for different experiments.
136
137 **Young and Old Chondrocyte Pools**
138 Chondrocytes at passage 0 (P0) were pooled with three to four other young chondrocyte donors
139 and grown in tissue culture flasks with GM at a cell seeding density of $1x10^6$ cells per flask. Media
140 was changed weekly. Once cells reached 80% confluency, cells were collected using
141 Trypsin/EDTA. Some cells were frozen using Recovery Cell Culture Freezing Medium (Gibco/
142 Thermo Fisher Scientific), and other cells were used for subsequent passaging. The same methods
143 were used for the old (> 45 years) chondrocyte pool. **Table S1** lists the chondrocyte ages and
144 genders used in each pool. Due to the extensive amount of work conducted using these pools, two
145 separate chondrocyte pools were made.
146
147 **RNA sequencing (RNA-Seq) and bioinformatics analysis**
148 The transcriptomic differences among three young and three old chondrocyte donors were assessed
149 through RNA-Seq. Individual chondrocyte cultures (P0) were lysed with the QIAzol reagent
150 (Qiagen, German Town, MD, United States), and RNA was isolated from the lysate using an RNA
151 Easy Plus Universal Kit (Qiagen). Extracted RNA were quantitated Qubit™ RNA BR Assay Kit
152 (Thermo Fisher Scientific) followed by the RNA quality check using Fragment Analyzer (Agilent
153 Technologies, Santa Clara, CA). For each sample, RNA libraries were prepared from 500ng RNA
154 using the KAPA mRNA HyperPrep Kit (Roche, Indianapolis, IN) according to manufacturer's
155 protocol, followed by quality check using Fragment Analyzer (Agilent Technologies) and

156 fluorescent quantification on the Infinite F Nano + (Tecan, Männedorf, Switzerland). The libraries
157 were normalized and pooled, and then sequenced using NovaSeq6000 platform (Illumina, San
158 Diego, CA,) to an average of 50M 100PE reads.
159 Quality control was first applied to raw RNA sequencing reads by tool FastQC. Low-
160 quality reads and adapter sequences were filtered out by the Trimmomatic tool. Surviving reads
161 were then aligned to human reference genome hg38 using STAR aligner, and gene counts were
162 quantified. Differential expression analysis was performed based on gene counts by R package
163 "DESeq2" and DEGs were selected by adjusted p-value < = 0.05 and fold change > = 1.5. These
164 DEGs were then applied to Ingenuity Pathway Analysis (IPA) to detect enriched pathways. This
165 software employs databases of prebuilt pathways with known genes summarized from previous
166 studies, checks the overlap between the DEG list and known pathways and performs statistical
167 tests to determine the enrichment. Significant pathways were defined by p-value < = 0.05.
168 Statistically stringently, FDR = 5% cutoff should be applied to control the false discovery rate. To
169 encourage more gene candidates, this study went by p-value< = 0.05 and fold-change> = 1.5 cutoff.
170 All the tools were run by default parameter settings.
171
172 **Immunohistochemistry (IHC) to examine the GATA4 levels in native cartilage tissues.**
173 Human cartilage tissues were fixed in 10% buffered formalin (Fisher Chemical, Fair Lawn, NJ) at
174 4°C overnight and then subjected to a graded ethanol dehydration series, starting from 20% ethanol
175 and progressing to 100% ethanol. Subsequently, they were embedded in Paraplast X-tra (Leica
176 Biosystems Inc. Richmond, IL). The Paraplast-embedded samples were sectioned at a thickness
177 of 6 µm using a rotary Leica microtome (Leica Microsystems Inc., Deerfield, IL, Model RM 2255).
178 Young and old mouse knee joints were gifts from Dr. Ana Mario Cuervo's lab at Albert Einstein
179 College of Medicine, which otherwise were wastes. After the specimens were fixed and decalcified
180 in a formic acid-based bone decalcifier (StatLab, Mckinney, TX, USA) for a period of two weeks,
181 they were then embedded and sectioned as described above.
182 For immunohistochemistry (IHC), the formalin-fixed paraffin-embedded sections first
183 underwent antigen retrieval based on different antibodies. Slides were then blocked with 10% goat
184 or horse serum (Abcam, Cambridge, MA) in phosphate buffered saline (PBS, Thermo Fisher
185 Scientific) for 1h, incubated at 4°C overnight with the primary antibody against GATA4, then
186 incubated with a biotinylated anti-mouse/rabbit immunoglobulin G(IgG) secondary antibody for

187 1h, with signal detection via DAB substrate kit (Abcam). The Nikon Eclipse E800 upright
188 microscope (Melivile, NY, United States) was used to image the stained sections. Antibody
189 specifications can be found in **Table S2**.
190
191 **Western blot to examine the GATA4 levels in human chondrocytes**
192 P1 young and old chondrocytes were used for individual chondrocyte analysis of GATA4. Cells
193 were washed in pre-cooled PBS (Thermo Fisher Scientific) three times. Using the RIPA buffer
194 (Sigma-Aldrich) supplemented with the protease and phosphatase Inhibitor Single-Use Cocktail
195 (Gibco/Thermo Fisher Scientific) and a cell scraper, monolayer culture samples were collected. A
196 pestle was used to homogenize pellets in the RIPA cocktail for pellet culture samples. The protein
197 concentration of the supernatant was determined by the Pierce™ BCA Protein Assay Kit (Thermo
198 Scientific). Proteins were fractioned electrophoretically on the NuPAGE 4-12%, Bis-Tris Mini
199 Protein Gel (Gibco/Thermo Fisher Scientific) and then transferred to a polyvinylidene fluoride
200 (PVDF) membrane using the iBlot Dry Blotting System (Invitrogen, Waltham, MA, United States).
201 The membrane was blocked with 3% non-fat milk (Bio-Rad, Hercules, CA, USA), diluted with 1×
202 Tris-buffered saline (TBS, Gibco/ Thermo Fisher Scientific) and 0.1% Tween 20 (Sigma-Aldrich)
203 (TBST) at room temperature for 1.5 h, washed, and incubated with the primary antibody at 4°C
204 overnight on a rotating shaker. The membrane was washed 7 times for 3 min with TBST buffer
205 and incubated with horseradish peroxidase (HRP)-linked secondary antibodies (GE Healthcare
206 Life Sciences, Malborough, MA, United States) for 1.5 h at room temperature. After being washed
207 5 times with TBST, the membrane was incubated in the chemiluminescence substrate SuperSignal
208 West Dura Extended Duration Substrate (Thermo Fisher Scientific). Images were acquired using
209 the ChemiDocTM Touch Imaging System (Bio-Rad). Images were quantified using ImageJ.
210 Antibody information is included in **Table S2**.
211
212 **Overexpression of *GATA4* in young human chondrocytes**
213 P2 young, pooled chondrocytes or young, individual chondrocytes were transduced with the
214 lentiviral vector containing *GATA4* fused with dTomato gene or the control lentivirus carrying
215 EGFP for 10 hours. After that, flasks were rinsed with PBS for 2 times and the medium was
216 replaced by fresh GM. Both vectors were created and packed by VectorBuilder (>10^8 TU/mL,
217 VectorBuilder, Chicago, IL, United States). To detect the number of cells transduced, cultures were

218 imaged with an EVOS M5000 microscope (Thermo Fisher Scientific) after 72 h of initial
219 transduction. After transduction, western blot, RT-qPCR, and IHC were used to verify the stable
220 expression of GATA4 in cells.
221
222 **RNA isolation and quantitative real-time polymerase chain reaction (RT-qPCR)**
223 For pellet culture, samples were first rinsed with PBS twice and a pestle and electric pulverizer
224 were used to crush pellets. Cells were homogenized in Qiazol (Qiagen). Total RNA was isolated
225 and purified using the RNAeasy Plus Universal Mini Kit (Qiagen, Cat. NO. 74104) according to
226 the manufacturer's protocol. The reverse transcription to the complementary DNA (cDNA) was
227 accomplished using the SuperScript IV VILO Master Mix (Invitrogen). RT-qPCR was performed
228 on a real-time PCR instrument (QuantStudio 3, Applied Biosystems, Foster City, CA, United
229 States) using the SYBR Green Reaction Mix (Applied Biosystems) with custom primers ordered
230 from Integrated DNA Technologies (IDT, Newark, NJ, United States). Relative gene expression
231 levels were calculated through the $2^{-\Delta\Delta Ct}$ method. Ribosomal protein L13A (*RPL13A*) was used as
232 the housekeeping gene. Full names and abbreviations of genes and their corresponding proteins
233 are listed in **Table S3,** and primer sequences are listed in **Table S4**.
234
235 **Pellet culture and chondrogenesis of young human Chondrocytes overexpressing *GATA4***
236 Following the lentiviral transduction of *GATA4* gene in young, pooled chondrocytes, the cells were
237 collected and formed into pellets at a cell seeding density of 3×10^5 cells per pellet. Pellets were
238 treated with chondrogenic medium (CM, DMEM with 1% v/v Insulin-Transferrin-Selenium-
239 Ethanolamine (ITS, Gibco/ Thermo Fisher Scientific), 1% antibiotic-antimycotics, 10^{-7} M
240 dexamethasone (Sigma-Aldrich), 40 µg/mL L-proline (Sigma-Aldrich), supplemented with 10
241 ng/mL transforming growth factor- β3 (TGF- β3, Peprotech, Rocky Hill, NJ, United States), and
242 50 µg/mL ascorbic acid-2-phosphate (Sigma-Aldrich)). Medium was changed daily for seven days.
243 RT-qPCR, histology, IHC, and western blot were used to characterize the tissues.
244
245 **Safranin O/Fast green staining**
246 Pellet samples were fixed in 10% buffered formalin (Fisher Chemical) for 2 h at room temperature
247 and then rinsed with PBS. Pellets then underwent serial dehydration in 30,50,70,95, and 100%
248 ethanol for one hour each. The 100% ethanol was refreshed once for an additional hour prior to

249 sample clearing in Xylene. Pellets were cleared in Xylene (Fisher Chemical) for two hours. Pellets
250 were then placed in Paraplast X-tra (Leica Biosystems Inc.) overnight. The next day, pellets were
251 embedded in Paraplast X-tra blocks and sectioned at a 6-µm thickness using a Leica microtome
252 (Leica Microsystems Inc., Model RM 2255).
253 Slides were stained using Safranin O (0.5%, Catalog number: 50240, Sigma-Aldrich), in 1%
254 acetic acid (Catalog number: A6283, Sigma-Aldrich), 0.005% fast green (0.05 g, Catalog number:
255 104022, Sigma-Aldrich) in 100 mL distilled water (Invitrogen) and counterstained with
256 Hematoxylin QS solution (Catalog number: H3404, Vector Laboratories INC). Imaging was
257 conducted using a Nikon Eclipse E800 upright microscope.
258
259 **LUMINEX multiplex assays**
260 Upon 7 days of chondrogenesis, condition medium from pellets was collected and flash frozen in
261 liquid nitrogen and immediately stored in -80^{oC}. LUMINEX assays were accomplished using the
262 Bio-Plex 200 system (Bio-Rad). Data collection and analysis were conducted using the Bio-Plex
263 Manager 6.1 software as established in previous studies.[19] LUMINEX kit information can be found
264 in **Table S5**.
265
266 **Knockdown of *GATA4* in old human chondrocytes**
267 The siRNA targeting human *GATA4* (ON-TARGET plus Human GATA4 (2626) siRNA, J-008244-
268 06-0005, Horizon Discovery Biosciences Limited, Cambridge, UK) was used in this study with a
269 scrambled siRNA (ON-TARGET plus non-targeting siRNA #1, Catalog number: D-001810-01-
270 05, Horizon Discovery Biosciences Limited) as the control. Old, pooled chondrocytes were
271 transfected with the siRNA using Lipofectamine RNAiMAX reagent (Thermo Fisher Scientific).
272 After 24 hours of incubation, the transfection medium (Opti-MEM Reduced Serum Medium,
273 Thermo Fisher Scientific) was changed to GM. Transfected cells were collected after 48 hours for
274 RT-qPCR to confirm the knockdown efficiency.
275
276 **Pellet culture and chondrogenesis of old human chondrocytes with *GATA4* Knockdown**
277 Following the 48h transfection of scrambled control siRNA or siRNA targeting *GATA4* , cells were
278 collected using Trypsin/EDTA (Thermo Fisher Scientific) and pellets were made at a cell density
279 of $3x10^5$ cells per pellet. Pellets were treated with CM supplemented with 10 ng/mL TGF- β3 and

280 50 μg/mL ascorbic acid-2-phosphate for 7 days. Upon day 7, pellets were collected for RT-qPCR,
281 western blot, and IHC.
282
283 **GATA4 Small Molecule NSC140905**
284 GATA4 small molecule, NSC140905, also known as HCA 42027(Biosynth Ltd, Compton, United
285 Kingdom), was reconstituted to 7.5 mM stock solution using UltraPure™ DNase/RNase-Free
286 Distilled Water (Invitrogen) on a shaker at 37° until completely dissolved. Old, pooled
287 chondrocytes were pelleted and treated with CM supplemented with 10 ng/mL TGF- β3 and 50
288 μg/mL ascorbic acid-2-phosphate with 100 μM NSC140905 for 14 days. Pellets were collected for
289 IHC, western blot, and RT-qPCR.
290
291 **Animal model**
292 All animal experiments were approved by the University of Pittsburgh Institutional Animal Care
293 and Use Committee (IACUC). Young (8 weeks) male C57BL/6 mice were purchased from Jackson
294 Laboratory (Bar Harbor, ME, USA) and maintained in pathogen-free conditions, with no more
295 than five mice per cage. Mice were provided ad libitum access to food and water, and a 12-hour
296 light/dark cycle to simulate natural circadian rhythms. To minimize bias, mice were randomly
297 assigned to either control or GATA4 groups, with 8 mice in each group.
298
299 **Intraarticular injection**
300 Intraarticular injections were administered to mice between 10-12 weeks of age under general
301 anesthesia to safeguard the well-being of the animals and to minimize procedural discomfort.
302 Under general anesthesia with 2% isoflurane in an oxygen mixture, the mice were placed in a
303 supine position, and the right knee joint was positioned at a 90-degree flexion to facilitate accurate
304 injection into the joint space. The injection site was meticulously identified medial to the patellar
305 tendon. Using a 29-gauge needle, a volume of 10 μL of lentiviral particles encoding either GATA4
306 or a control vector (at a concentration $>10^8$ TU/mL, VectorBuilder) was precisely administered
307 into the intra-articular space of the right knee. The precision of the injection was ensured by
308 employing a consistent technique across all animals, thereby reducing variability in the delivery
309 of the viral vectors.
310

311 **Destabilization of the medial meniscus (DMM) surgery**

312 One week after viral vector injection, DMM surgery was performed to induce the OA model on
313 mice at 11-13 weeks of age.[20,21] Briefly, a medial parapatellar incision was made to expose the
314 right knee joint, followed by a careful opening of the joint capsule. The anterior medial menisco-
315 tibial ligament was identified and transected using microscissors. The joint capsule and skin were
316 subsequently sutured with 6-0 silk thread. For experimental controls, a sham operation was
317 performed in which the joint capsule was exposed as in the DMM surgery, but the medial menisco-
318 tibial ligament was left intact.

319

320 **Knee hyperalgesia**

321 We expected accelerated OA development after *Gata4* overexpression. To observe these
322 differences, we used six weeks as the time point at which control mice had begun displaying mild
323 OA symptoms. Knee hyperalgesia was evaluated using a Pressure Application Measurement
324 (PAM) device (Ugo Basile, Varese, Italy).[22,23] Mechanical stimuli were applied to the mouse's knee
325 joint to assess the degree of hyperalgesia based on the applied pressure and the mouse's response.
326 Six weeks after either DMM or sham surgery, the mice were carefully removed from their cages
327 to ensure they remained calm and unstimulated. The mouse was held securely by its back to
328 maintain a straight posture, with the right knee joint flexed at approximately 90 degrees. The PAM
329 device was placed on the index finger of the right hand of testers, which, along with the thumb,
330 was used to apply pressure to the medial side of the knee joint, ensuring proper contact. Pressure
331 was gradually applied at a constant rate of 30 g/s while monitoring the pressure curve displayed
332 on the computer. The sensor was released immediately when the mouse exhibited a response to
333 the applied stress, such as head movement, vocalization, or knee withdrawal. The pressure value
334 displayed by the software, and the maximum pressures that mice can withstand were recorded.
335 Two measurements were taken per knee, one on the medial side, and one on the lateral side the
336 average was calculated for accuracy.

337

338 **Synovial inflammation score**

339 After 6 weeks, knee joints were collected and sectioned as described above. Histology staining
340 and IHC were used to assess OA severity. Synovial inflammation score was evaluated according

to a scoring protocol outlined in previous studies[24], which relies on the hematoxylin and eosin (H&E)-stained tissue sections.

Statistical Analysis

Each experiment was carried out with at least three biological replicates. Data is presented as mean ± standard deviation unless otherwise specified. Detailed information of sample size, pre-processing, and statistical methods have been specified in each figure legend. Prism 10 (GraphPad, San Diego, CA) was used for statistical analysis. The significance level was set at 0.05 and indicated by * ($p < 0.05$), ** ($p < 0.01$), *** ($p < 0.001$), and **** ($p < 0.0001$).

351 **Results**

352 *GATA4 is predicted to regulate chondrocyte aging*

353 To limit the influence of *in vitro* expansion on cell phenotype, P0 human chondrocytes
354 were used for RNA sequencing (**Figure 1A**). The volcano plot showed that 303 genes are
355 upregulated and 163 genes are downregulated in aged chondrocytes compared to young cells
356 (**Figure 1B**). The top 50 most changed genes are listed in **Figure 1C**. Interestingly, the
357 osteoarthritis pathway was identified to be activated in old chondrocytes (**Figure 1E**).

358 Through Ingenuity Pathway Analysis (IPA) Upstream Regulator Analysis, transcriptional
359 regulators that may mediate the difference between young and old cells were predicted, and the
360 top 20 of them are shown in **Figure 1D**. Given that GATA4 was previously shown to regulate
361 chondrocyte senescence[13] and be involved in the activation of Nuclear Factor Kappa B (NF-κB)
362 pathway in tissues like the nucleus pulposus[25] and synovium,[26,27] it was selected for further
363 investigation in this study. Initial data analysis predicted that GATA4 was upregulated in aged
364 chondrocytes compared to young donors (**Figure 1D**). Immunohistochemistry (IHC) results
365 indicated that GATA4 was more abundant in articular cartilage harvested from aged individuals
366 (**Figure 1F**) (**Supplementary Figure S1**). Analyzing knee joints collected from young and old
367 mice also demonstrated that GATA4 levels were higher in aged cartilage tissues compared to young
368 (**Supplementary Figure S2**). To further confirm the findings, western blot was used to examine
369 GATA4 levels in isolated chondrocytes, and the results indicated that aging correlates with the
370 increase of GATA4 in chondrocytes (**Figure 1G**).

371

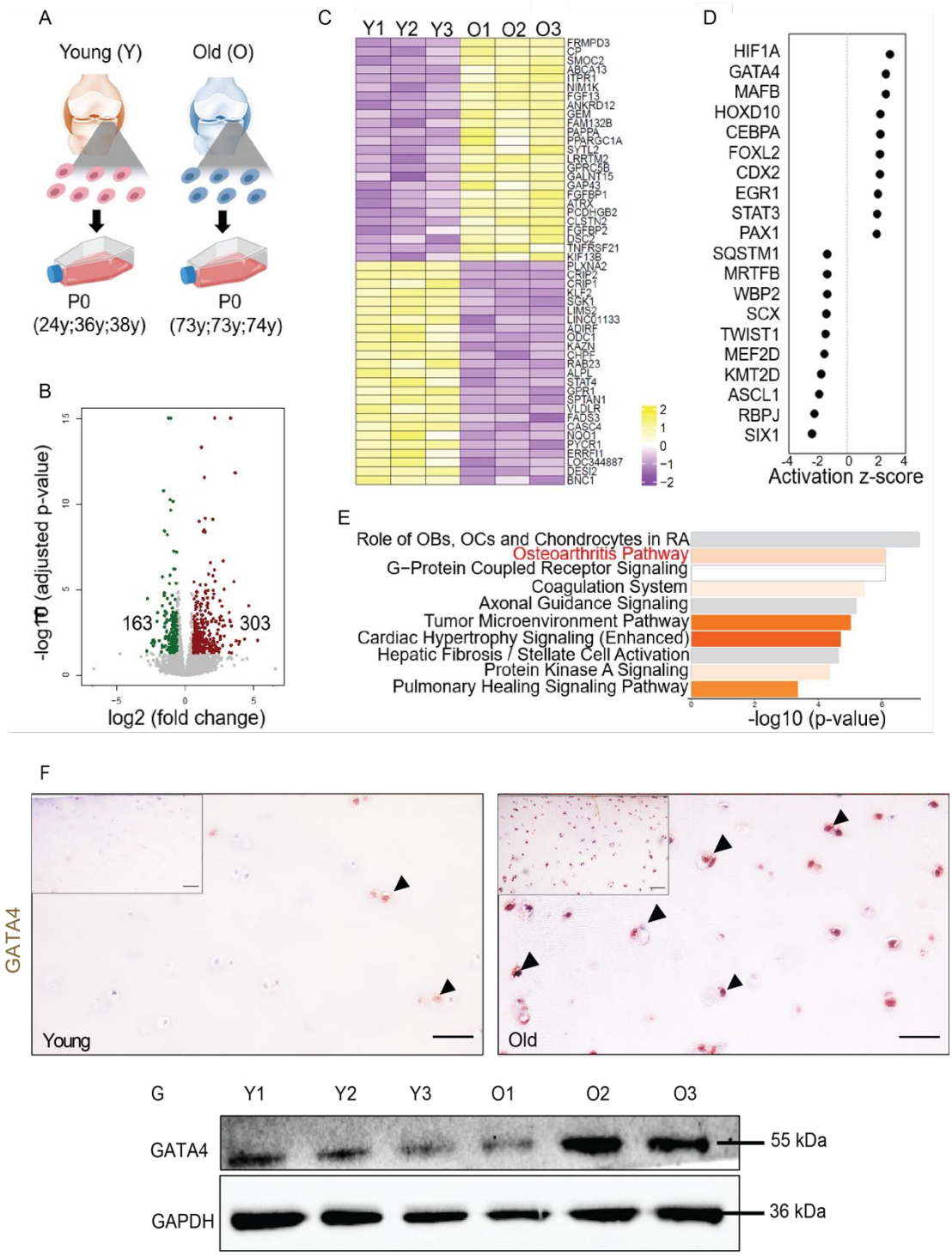

***Figure 1**: **GATA4 is predicted to regulate chondrocyte aging.** (A) Healthy chondrocytes were isolated from knee joint cartilage from young and old donors without osteoarthritis (assessed by experienced surgeons). P0 cells were used for RNA sequencing analysis. (B) Volcano plot demonstrating 303 upregulated and 163 downregulated genes in old chondrocytes when compared*

377 *to young cells. (C) Top 50 genes that are significantly differently expressed in young and old*
378 *chondrocytes. (D) Activation Z score of top 10 transcription regulators that are activated (positive)*
379 *or inhibited (negative) in aged versus young chondrocytes. A comprehensive list of gene names*
380 *can be found in* ***Table S3****. (E) Ingenuity Pathway Analysis (IPA) of young versus old cells. The*
381 *gray bars indicate that no activity pattern is identified in IPA despite the highly significant*
382 *association of the genes within the pathway. Orange, positive z-score; white, zero z-score.*
383 *OBs=osteoblasts; OCs=osteoclasts. (F) GATA4 IHC of healthy human cartilage tissue from young*
384 *and aged donors. Bar=50 µm. (G) Relative protein levels of GATA4 in P1 chondrocytes from*
385 *individual human donors were analyzed by western blot.*
386
387 *Overexpressing GATA4 impairs the hyaline cartilage formation capacity of young chondrocytes*
388 To examine the functions of GATA4 in chondrocytes, we first overexpressed it in healthy
389 young human chondrocytes (**Figure 2A**). Real-time quantitative PCR (RT-qPCR),
390 immunostaining, and western blot confirmed the significantly increased GATA4 expression after
391 infection, which did not impact the expression levels of collagen type II (COLII)-α1 (*COL2A1*)
392 and aggrecan (*ACAN*), but significantly upregulated the expression of Collagen type X (COLX)-
393 α1 (*COL10A1*) and India hedgehog (IHH), two representative chondrocytic hypertrophy markers
394 (**Supplementary Figure S3**). We then examined the cartilage formation capacity of cells by
395 culturing cells in chondrogenic medium for 7 days. IHC, RT-qPCR, and western blot demonstrated
396 the continuous overexpression of *GATA4* in newly formed tissues (**Figure 2B-D**). Interestingly,
397 significantly reduced GAG and COLII production was found in the overexpression *GATA4* group
398 (GATA4 group) compared to the GFP control group (**Figure 2E-G**). Similar results were observed
399 in the study testing chondrocytes from individual donors (**Supplementary Figure S4**).
400 Interestingly, *GATA4* overexpression did not impact the expression of *COL10A1* and *IHH* in the
401 cartilage pellets **(Figure 2G**). Additionally, tissues from the GATA4 group secreted more
402 proinflammatory cytokines, including IL-6, IL-8, TNF-α, and chemokine CCL2 (**Figure 2H&I**),
403 as well as enzymes that can break down cartilage, including matrix metalloproteinases *(MMP)-1,*
404 *2, 12*, and a disintegrin and metalloproteinases *(ADAMTS) 5* (**Figure 2J&K**). Although the
405 expression levels of *MMP-13* gene decreased in GATA4 group, the protein levels showed no
406 difference between the two groups (**Supplementary Figure S5**).

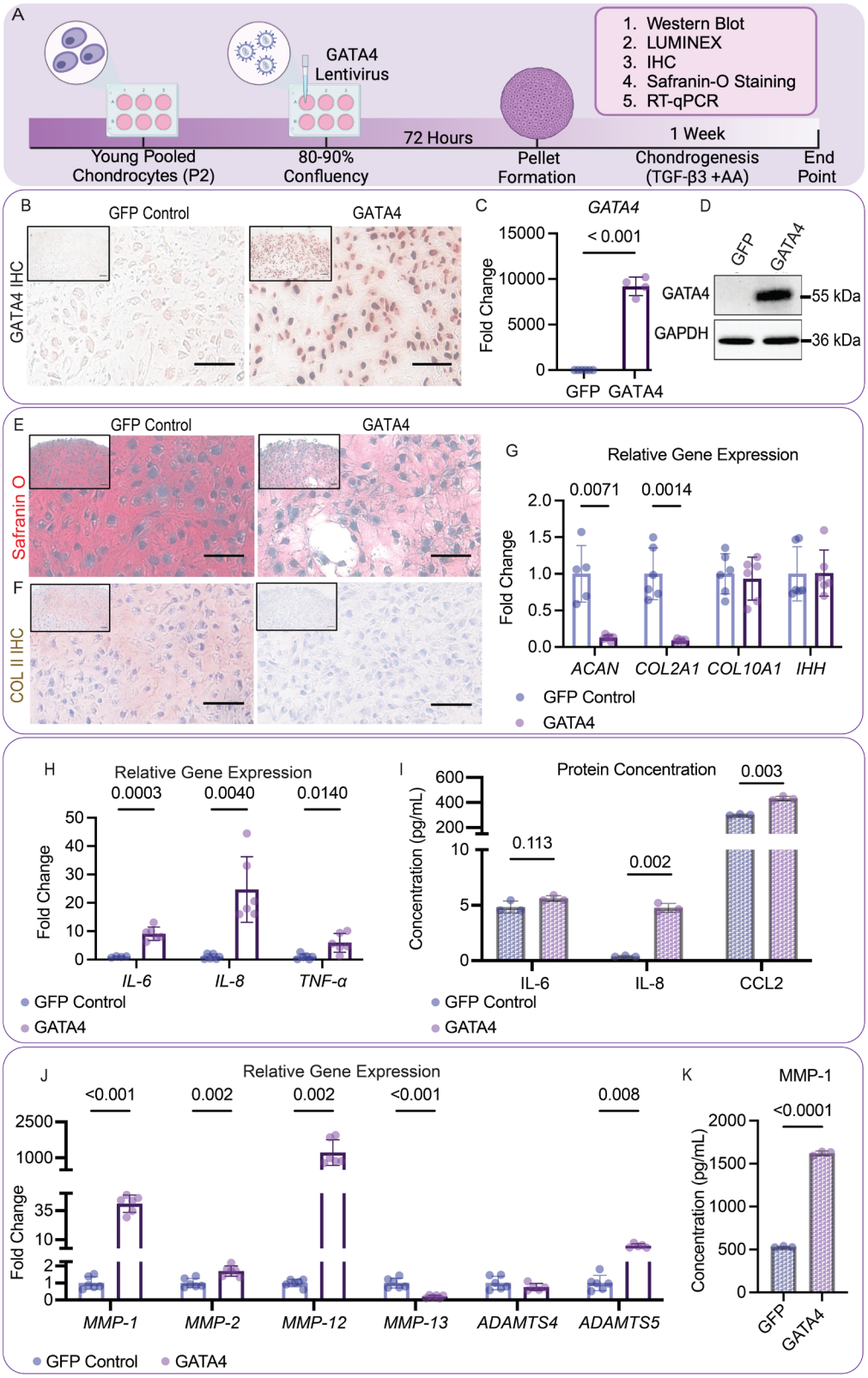

407

408 ***Figure 2: Overexpressing GATA4 impairs the hyaline cartilage formation capacity of young***
409 ***chondrocytes.*** *(A) Timeline depicting the study. (B) IHC to assess GATA4 protein levels in young*

410 *cells overexpressing GFP control or GATA4. Scale Bar=50 µm. (C) RT-qPCR analysis of GATA4*
411 *gene expression in two groups. (D) Western blot to measure GATA4 protein levels. (E) Safranin O*
412 *staining and (F) Collagen type II (COLII) IHC to examine the production of cartilage matrix.*
413 *Scale Bar=50 µm. (G) RT-qPCR analysis of gene expression of cartilage matrix proteins aggrecan*
414 *(ACAN) and collagen type II-α1 (COL2A1) and hypertrophy markers collagen type X- α1*
415 *(COL10A1) and India hedgehog (IHH). (H) RT-qPCR analysis of gene expression of*
416 *proinflammatory cytokines, including interleukin (IL)-6, IL-8, and tumor necrosis factor- α* (*TNF-*
417 *α*) (n=6). *(I) Concentrations of IL-6, IL-8, and chemokine (C-C motif) ligand 2 (CCL2) in condition*
418 *medium* (n=3). (*J) RT-qPCR analysis of relative gene expression of matrix-degrading enzymes,*
419 *including matrix metalloproteinases (MMP)-1,2,3,12, and 13, and a disintegrin and*
420 *metalloproteinase (ADAMTS) 4 and 5* (n=6). *(K) MMP-1 concentration in condition medium*
421 (n=3). *Student's two-tailed t-test with Welch's correction for standard deviation and a p-value of*
422 *0.05 was used for all statistical analysis. Created in BioRender. Makarczyk, M. (2025)*
423 *https://BioRender.com/luon9t1*
424
425 *GATA4 overexpression activates SMAD1/5*
426 Increased SMAD1/5 phosphorylation represents a key feature of aged chondrocytes [28]. We
427 thus examined whether increased GATA4 levels are associated with SMAD1/5 activation (**Figure**
428 **3A**). In the experiment testing chondrocytes from individual donors (**Figure 3B, D-G**),
429 overexpression of GATA4, even without the stimulation of TGF-β3, was sufficient to activate
430 SMAD1/5, but not SMAD2/3. In addition, the group that was co-treated with GATA4
431 overexpression and TGF-β3 displayed the highest phosphorylated SMAD1/5 (pSMAD1/5) levels
432 in all tested groups. Of note, activation of SMAD2/3 was not impacted by GATA levels. A similar
433 trend was also observed in the study using pooled chondrocytes (**Figure 3C**).
434

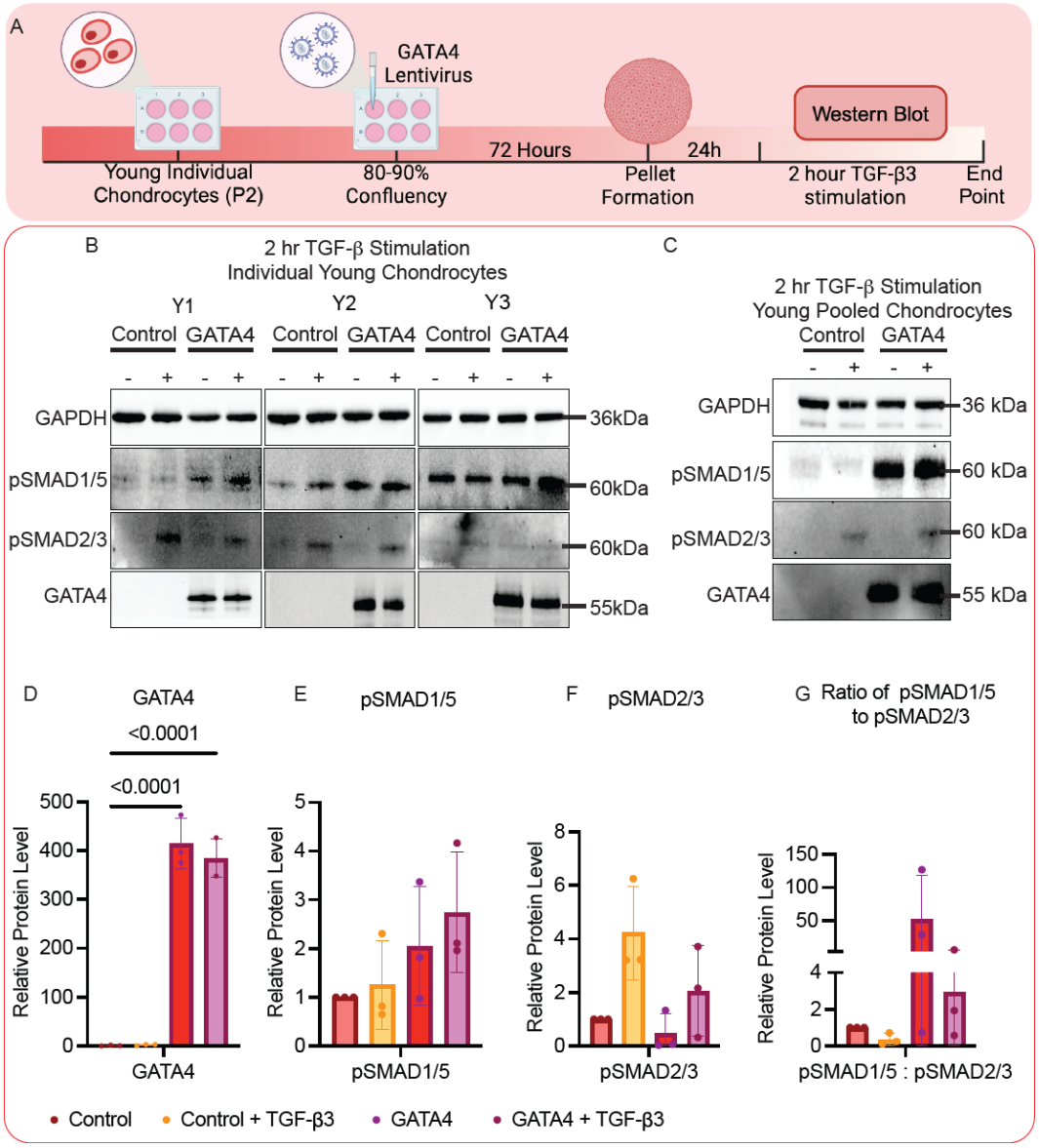

Figure 3 GATA4 overexpression activates SMAD1/5. *(A) Schematic showing the experiment.* ***(B,*** *C) Western blot to assess protein levels of phosphorylated SMAD1/5 (pSMAD1/5), phosphorylated SMAD2/3 (pSMAD2/3), and GATA4 in pellets derived from young (B)individual(Y1-3) or (C) pooled chondrocytes, which were infected with lentiviral vectors carrying GATA4 or control genes and then stimulated with (+) or without (-) TGF- β3 for two hours. Relative protein levels of (D)GATA4, (E)pSMAD1/5, and (F)pSMAD2/3 were semi-quantified using ImageJ (n=3). (G) The ratio of pSMAD1/5 compared to pSMAD2/3 was also calculated. Statistics were conducted using one-way Analysis of Variance (ANOVA) with Dunnett's post hoc analysis. Created in BioRender. Makarczyk, M. (2025) https://BioRender.com/luon9t1*

445 *Suppressing GATA4 in old chondrocytes promotes ECM formation and lowers proinflammatory*
446 *cytokines*

447 We then tested the potential of suppressing GATA4 in reversing chondrocyte aging (**Figure**
448 **4A**). Several GATA4 siRNAs were tested to examine their capacity to suppress *GATA4*. Based on
449 RT-qPCR results, siRNA2 was selected to be used in all following studies because it induced the
450 lowest expression of *GATA4*. (**Supplementary Figure S6**). *GATA4* knockdown resulted in
451 increased cartilage formation from old chondrocytes, which did not influence the expression of
452 hypertrophy marker *COL10A1* (**Figure 4B-D**). Moreover, although we did not see a difference
453 between the scrambled control and GATA4 siRNA groups regarding the expression of *IL-6* and
454 *IL-8*, the protein level of IL-8 was higher in the GATA4 group. Interestingly, the protein level of
455 CCL2 was significantly decreased after GATA4 knockdown (**Figure 4E, F**). We also tested the
456 expression levels of MMPs and ADAMTSs (**Figure 4H-I**). In general, suppressing GATA4 either
457 decreased or caused no significant changes to the levels of these enzymes. In particular, MMP-13
458 levels were reduced, in both gene and protein levels (in condition medium), after GATA4
459 knockdown. Mechanistically, GATA4 siRNA treatment also lowered the phosphorylation of
460 SMAD1/5 and p-P65 (**Figure 4G**).

461 In a separate study, we used a small-molecule GATA4 inhibitor NSC140905, which was
462 shown to significantly promote cartilage formation from old chondrocytes and reduce the
463 expression of proinflammatory cytokines (**Supplementary Figure S7**). Taken together,
464 suppressing GATA4 partially restored the capacity of old chondrocytes to create new cartilage.
465

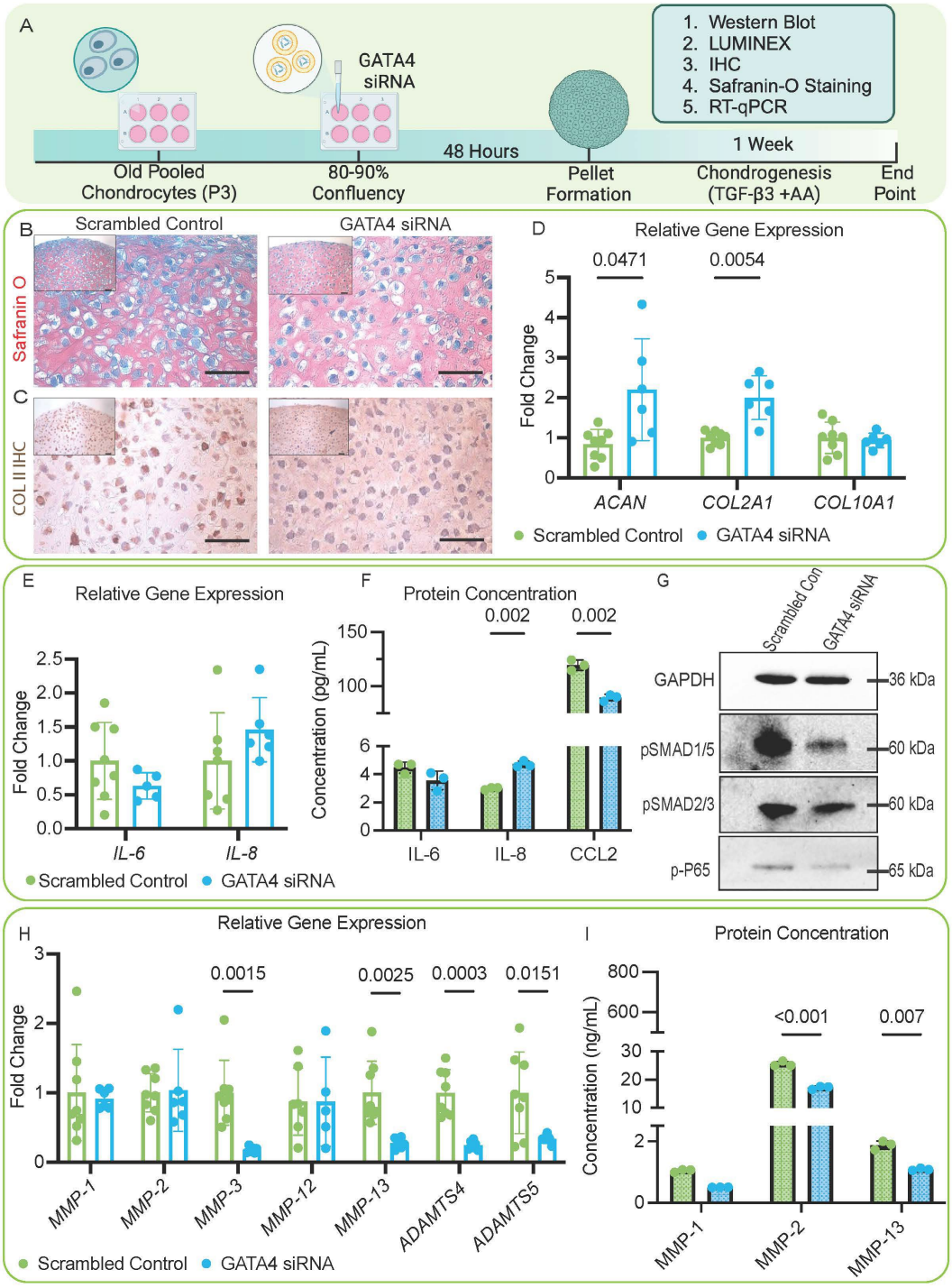

Figure 4: Influence of GATA4 knockdown on in vitro cartilage formation of old chondrocytes. *(A) Schematic showing the study. (B) Safranin O staining and (C) COLII IHC to examine the production of cartilage matrix in the Scrambled Control or GATA4 siRNA group. Scale Bar=50 µm. (D) RT-qPCR analysis of relative gene expression of cartilage matrix proteins ACAN and COL2A1 and hypertrophy marker COL10A1*(n=6). *(E) RT-qPCR analysis of relative gene*

expression of proinflammatory cytokines IL-6 and IL-8 (n=6). (*F*) *Concentrations of IL-6, IL-8, and chemokine (CCL2) in condition medium* (n=3). (*G) The relative protein levels of pSMAD1/5, pSMAD2/3, and phosphorylated p65 (p-P65) in two groups. (H) RT-qPCR analysis of relative gene expression of matrix-degrading enzymes, including MMP-1,2,3,12, and 13, and ADAMTS 4 and 5* (n=6). *(I) MMP-1,2 and 13 concentrations in condition medium* (n=3). *Student's two-tailed t-test with Welch's correction for standard deviation and a p-value of 0.05 was used for all statistical analysis. Created in BioRender. Makarczyk, M. (2025) https://BioRender.com/luon9t1*

Gata4 overexpression in the knee joints accelerates OA progression in mice

The physiological functions of GATA4 were further examined using a mouse model (**Figure 5A**). Specifically, lentiviral vectors carrying *Gata4* or *mCherry* genes were injected into the knee joints of young mice. One week after the injection, DMM surgery was conducted to induce OA. Since we expected that Gata4 overexpression would accelerate OA progression, we harvested samples for analysis 6 weeks after DMM.

Results from IHC indicated a successful Gata4 overexpression in hyaline cartilage even 6 weeks after injection (**Figure 5B, C**). Interestingly, mice overexpressing Gata4 in the knee joint resulted in the elevation of p-P65 (**Figure 5D, E**), suggesting increased inflammation. Moreover, the mice in the Gata4 group displayed more severe OA and higher knee hyperalgesia than the control group, as revealed by a lower withdrawal threshold. (**Figure 5F-H**). Interestingly, mice from the Gata4 group displayed higher synovial inflammation (**Figure S8**).

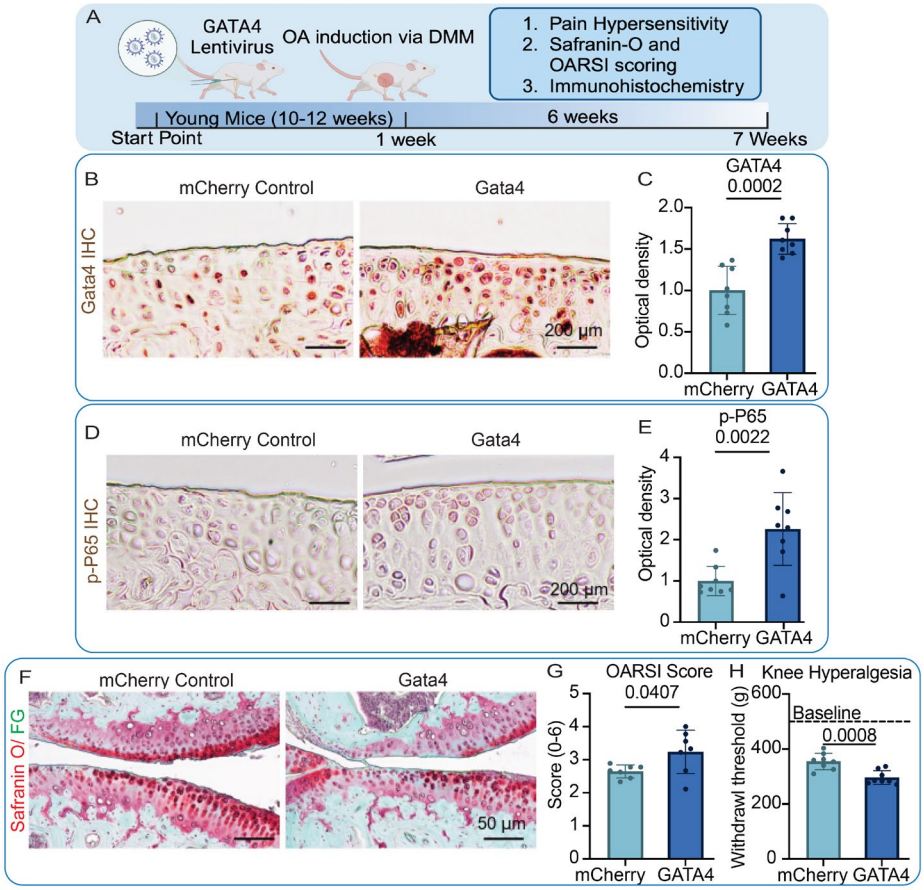

Figure 5: Gata4 overexpression in the knee joints accelerates OA progression in mice. *(A) schematic of the study. Mice received one intraarticular injection of lentiviral vectors that carried mCherry or Gata4 gene one week before DMM surgery was performed. Knee joints were harvested 6 weeks post-surgery. Levels of Gata4 (B, C) and p-P65 (D, E) were assessed with IHC(B&D), and the staining was semi-quantitated with Image J (C&E). Cartilage degradation was assessed with (F) Safranin O/ fast green (FG) staining, and (G)OARSI score was calculated. (H)Knee hyperalgesia 6 weeks post-surgery. 507 g was the threshold baseline for non-surgery mice (dashed line). Student's two-tailed t-test with Welch's correction for standard deviation and a p-value of 0.05 was used for all statistical analysis. Created in BioRender. Makarczyk, M. (2025) https://BioRender.com/luon9t1*

Discussion

The causal relationship between aging and OA has been documented, and understanding the molecular mechanisms is essential for the development of treatment methods. In this study, we discovered the critical roles of aging-associated increases in GATA4 levels. Specifically,

508 overexpressing GATA4 in young chondrocytes impaired their capacity to form normal hyaline
509 cartilage, while suppressing GATA4 in old chondrocytes restored their chondrogenic potential. We
510 also demonstrated that GATA4 functions partially by promoting the activation of SMAD1/5. Our
511 *in vivo* work further confirmed that high *Gata4* expression accelerated OA progression in mice.
512 Lastly, we defined a small-molecule GATA4 inhibitor that can partially restore the capacity of old
513 chondrocytes to create healthy cartilage, representing a potential DMOAD for further validation
514 in the future.

515 Given the recognized challenges in harvesting healthy cartilage tissues from donors without
516 arthritis, there are limited reports investigating chondrocyte aging per se. The current findings
517 include proliferation and post-expansion chondrogenic capacity reduction with aging,[29] increased
518 MMP-13 production in response to catabolic stimuli,[30] and altered response to TGF-β.[12] One of
519 our recent studies again demonstrated that aged chondrocytes displayed a reduced proliferation
520 potential compared to young cells. Additionally, cartilage tissues generated by old chondrocytes
521 contained more senescent cells than those from young cells.[31] However, to the best of our
522 knowledge, there were no publications describing the transcriptomic comparisons between young
523 and old chondrocytes, which would be informative in defining targets to stop or reverse
524 chondrocyte aging.

525 Through transcriptomic analysis, we were able to assess the expression of different genes and
526 genetic pathways that occur as chondrocytes age. Of note, Hypoxia-Inducible Factor 1α (HIF1α)
527 was the most differentially expressed gene predicted to regulate chondrocyte aging. The
528 connection between HIF1α and aging has been previously reported.[32] Furthermore, additional
529 studies have investigated HIF1α in association with OA and assessed its use as a therapeutic
530 target.[33,34] Therefore, we decided to focus on GATA4, which was less studied in chondrocytes but
531 highly associated with cellular senescence, an aging hallmark. However, our selection did not
532 dampen the importance of HIF1α and other molecules listed in Figure 1D in chondrocyte aging.
533 They can be further studied in the future using the same strategy employed in the current work.

534 The GATA family consists of several proteins (GATA1-6) with different variations of
535 DNA-binding domains composed of zinc finger structures.[25] Particularly, GATA4, 5, and 6 are
536 involved in the development of the mesoderm and endoderm tissues,[35] in which GATA4 has been
537 detected in the development of structures such as the heart,[36,37] pancreas,[38] lung, and liver.[39,40] In
538 addition, GATA4 and GATA6 are the only members that are associated with aging.[41] Particularly,

539 GATA4 is unique in that it regulates tissues in a context-dependent manner and adopts a
540 multifaceted role in the body, contributing to other age-related diseases such as atherosclerosis[42]
541 and heart failure.[43]

542 Furthermore, GATA4 might be associated with metabolic regulation. A study conducted by
543 Patankar et al. investigated how GATA4 regulates obesity. Specifically, they used intestine-specific
544 *Gata4* knockout mice to study diet-induced obesity, showing that the knockout mice were resistant
545 to the high-fat diet, and that glucagon-like peptide-1 (GLP-1) release was increased. These findings
546 indicated a decreased risk for the development for insulin resistance in knockout mice.[44] This work
547 was taken a step further in a subsequent publication, in which the same team investigated the
548 dietary lipid-dependent and independent effects on the development of steatosis and fibrosis in
549 *Gata4* knockout mice. The results from this work suggested that the knockdown of *Gata4* increases
550 GLP-1 release, in turn suppressing the development of hepatic steatosis and fibrosis ultimately
551 blocking hepatic *de novo* lipogenesis.[45] These studies are especially interesting with the rise of
552 GLP-1 based therapy for the treatment of OA.[46,47] Thus, the coupling of GATA4-related metabolic
553 dysfunction and OA should be further investigated.

554 In 2015, GATA4 was first introduced as a senescence regulator in a study conducted by
555 Kang et al.[13] This work demonstrated the role of GATA4 in human fibroblasts and determined that
556 the inhibition of autophagy caused GATA4 accumulation following DNA damage. They examined
557 the presence of GATA4 in the human brain and found that there was an increase of GATA4 in the
558 prefrontal cortex of aged human samples.[13] Further studies have shown that GATA4 regulates
559 angiogenesis and inflammation in fibroblast-like synoviocytes in rheumatoid arthritis, indicating
560 that GATA4 is required for the inflammation induced by IL-1β. This study also demonstrated that
561 GATA4 binds to promoter regions on Vascular Endothelial Growth Factor (VEGF)-A and VEGFC
562 to enhance transcription and regulate angiogenesis.[15] In chondrocytes specifically, previous studies
563 demonstrated that increased GATA4 levels are associated with chondrocyte senescence,[17,48,49] an
564 important change often observed in OA chondrocytes. Moreover, suppressing GATA4 with siRNA
565 was shown to effectively abolish ionizing radiation-induced senescent phenotype in
566 chondrocytes.[17] Of note, all these studies relevant to chondrocytes were conducted *in vitro.* Herein,
567 we, for the first time, demonstrate the role of GATA4 in regulating chondrocyte aging.

568 A theory of chondrocyte aging proposed by van der Kramm suggests that alterations to the
569 TGF-β pathway induce chondrocyte hypertrophy and result in articular cartilage that is prone to

570 OA development.[12] While investigating the function of GATA4 in chondrocytes, we assessed how
571 its levels contribute to TGF-β alterations in chondrocytes and found that GATA4 levels negatively
572 correlated with the anabolic potential of chondrocytes (**Figures 2 and 4**). Our study indicated that
573 there was an observed decrease in chondrogenesis and an increase in hypertrophy-related genes
574 following *GATA4* overexpression (**Figure 2G)**. To maintain healthy cartilage homeostasis,
575 numerous pathways are involved. In particular, TGF-β is a crucial cytokine necessary for cartilage
576 homeostasis during OA,[50,51] and aged chondrocytes respond differently to TGF-β compared to
577 their young counterparts.[52]

578 Mechanistically, in the TGF-β pathway, TGF-β binds to the heterotetrameric receptor complex,
579 which can be grouped into three receptor types (type I, type II, and type III). When TGF-β binds
580 to its corresponding receptor, the activin-receptor-like kinases (ALKs) are activated.[53] Typically,
581 the anabolic binding of TGF-β to ALK4/5 results in the phosphorylation of SMAD2/3, protecting
582 chondrocytes from hypertrophy.[50] However, there can also be catabolic effects associated with the
583 expression of SMAD1/5, typically expressed when TGF-β binds to ALK1/2/3/6.[50,53] The
584 phosphorylation of SMAD1/5 results in the promotion of ECM degrading proteins such MMP-
585 13.[28,50] As mentioned previously, research has demonstrated that aged chondrocytes respond
586 differently to TGF-β compared to young chondrocytes.[52,54] Chondrocyte aging has been linked to
587 the increase of pSMAD1/5 signaling.[28] These previous studies and literature review inspired us to
588 explore the potential association between GATA4 levels and the activation of SMAD1/5.

589 Our results found that GATA4 resulted in the phosphorylation of SMAD1/5 even without TGF-
590 β stimulation, which however did not alter the phosphorylation of SMAD2/3. Although there are
591 no current publications specifying the complex relationship of GATA4 and SMAD1/5 in
592 chondrocytes, a prior study reported that GATA4 was regulated by SMAD1/5. Specifically,
593 SMAD1/5 and GATA4 can bind together to promote IL-6 expression in macrophages.[55] In this
594 study, it was shown that GATA4 was necessary for bone morphogenic protein-6 (BMP-6) mediated
595 IL-6 induction, in which there are multiple GATA binding domains on the IL-6 promoter. This
596 work further showed that GATA4 interacts with SMAD 2,3 and 4.[55] Studies have suggested that
597 BMP pathways and GATA4 work synergistically to regulate SMAD signaling.[56] This information
598 indicates that the involvement of GATA4 in the TGF-β signaling pathway is complex, and further
599 studies should be conducted to better assess this relationship.

600 Additionally, a common hallmark of chondrocyte aging is the alternation of ECM,
601 including composition change[2] and stiffening.[57] ECM stiffness can directly affect chondrocyte
602 phenotype and proliferation, and contribute to OA.[58] A recent study by Fu et al. associated matrix
603 stiffening with the promotion of chondrocyte senescence.[59] Furthermore, matrix stiffening has
604 been associated with modulating the TGF-β signaling pathway.[60-62] Future studies should
605 investigate the potential of matrix stiffening and the effect of GATA4 on pericellular matrix
606 proteins such as decorin[63,64], biglycan, collagen VI and XV, as these proteins assist with the
607 regulation of biochemical interactions and assist with the maintenance of the chondrocyte
608 microenvironment.[65] Herein, the TGF-β signaling pathway can further alter the extracellular
609 microenvironment[62], which could promote cellular senescence and subsequently NF-κB pathway
610 activation.

611 While the TGF-β pathway is closely associated with cartilage matrix remodeling, we also
612 found increases in the levels of multiple proinflammatory cytokines after GATA4 overexpression.
613 We investigated the NF-κB pathway since it is also activated in aged tissues.[66,67] During the aging
614 process, NF-κB is thought to amplify and potentially propagate cellular senescence through the
615 senescence-associated secretory phenotype (SASP).[16] A study by Qiao et al. indicated that GATA4
616 regulates NF-κB in dental pulp cells[14] and fibroblasts[15]. Specifically, using siRNAs, they
617 determined that the knockdown of GATA4 decreased p65 production induced by
618 lipopolysaccharide (LPS).[14] Other studies have investigated the role of GATA4 in the synovium
619 and the progression of the disease state of rheumatoid arthritis and OA. Jia et al. showed that the
620 knockdown of GATA4 attenuated synovial inflammation and joint damage in a collagenase-
621 induced arthritis mouse model.[15] More recently, a study conducted by Chen et al. investigated the
622 roles of GATA4 in fibroblast-like synoviocytes (FLS) and determined that GATA4 induced cellular
623 senescence in FLSs in OA progression.[27] Our study also discovered that the siRNA knockdown of
624 GATA4 decreased the phosphorylation of p65 in aged chondrocytes (**Figure 4**). However, we also
625 noticed that MMP-13 expression levels decreased in both *GATA4* overexpression and knockdown
626 experiments. It should be noted that MMP-13 is constitutively produced in human chondrocytes
627 but is only activated under pathological conditions. Given that MMP-13 is regulated by different
628 transcriptional factors and cytokines, as well as RNAs,[28] its associations with GATA4 require
629 further investigation in the future. Collectively, these findings further indicate that GATA4 might
630 regulate aging partially through TGF-β and NF-κB pathways.

631 Our current study has not fully explored why aging promotes GATA4 expression. The study
632 from Kang et al. indicated that DNA damage contributed to GATA4 accumulation.[13] It is known
633 that DNA damage response (DDR) is regulated by ataxia telangiectasia mutated (ATM) and ataxia
634 telangiectasia and Rad3–related (ATR) signaling.[13,68,69] The activation of these signaling pathways
635 inhibits autophagy-related protein p62.[70] In addition, Copp et al. reported increased DNA damage
636 in old chondrocytes.[5] These studies implied that DNA damage may be a reason for GATA4
637 upregulation. Our preliminary data and prior work from Kan et al.[13] support this possibility.
638 Specifically, a DNA damage-inducing agent, doxorubicin, promoted the upregulation of GATA4
639 in chondrocytes (**Supplementary Figure S9**). To further link DNA damage to GATA4
640 accumulation, a study by Chung et al. used Tributyltin (TBT), a well-known endocrine-disrupting
641 chemical, to induce DNA damage in articular chondrocytes. After 24 hours of TBT treatment, there
642 was a significant increase in *GATA4* expression and expression of senescence markers.[48] The study
643 by Kang et al. demonstrated that the suppression of p62 following DNA damage leads to GATA4
644 accumulation due to the lack of autophagy.[13] DNA damage is known to increase with age.[71]
645 Therefore, we believe that DNA damage due to aging is a key driver of the upregulation of GATA4
646 in old chondrocytes.
647 In conclusion, we have determined that GATA4 is increased in aged chondrocytes
648 compared to young in both humans and mice, which may be induced by increased DNA damage
649 observed in aged cells. We also demonstrated that GATA4 overexpression impaired the quality and
650 quantity of cartilage created by chondrocytes and accelerated OA progression in mice. Conversely,
651 suppressing GATA4 with siRNA or small-molecule inhibitors partially restores the capacity of old
652 chondrocytes to form cartilage. Additionally, our study found that GATA4 can activate SMAD1/5
653 and change chondrocyte response to TGF-β. Overall, our study indicated that GATA4 could be a
654 contributor to OA onset and progression in aged individuals, which can also serve as a potential
655 target to prevent aging-associated OA.
656 There are some limitations of this study that can be further addressed in future studies. First,
657 this study has allowed us to examine the potential mechanisms of GATA4 in chondrocyte aging.
658 Although we found that GATA4 was generally increased with aging, some young donors also
659 exhibited increased levels of GATA4, which may be associated with increased DNA damage, as
660 discussed above, or other stressors. Therefore, GATA4 should be used together in conjunction with
661 other aging biomarkers, such as epigenetic clock [72] to precisely define chondrocyte aging. Future

662 work should examine biological versus chronological aging and epigenetic clock-based
663 assessments to explain the variabilities in GATA4 expression among donors. Second, the TGF-β
664 signaling pathway is complex, and there are multiple studies that have associated it with GATA4.
665 However, the relationship between GATA4 overexpression and SAMD1/5 activation should be
666 further investigated to elucidate specific signaling mechanisms. Third, during our *in vivo* work,
667 the intraarticular injection of GATA4 lentivirus was not chondrocyte-specific. Therefore, the
668 injection also allowed for other cell types to overexpress GATA4. Future work should be conducted
669 using transgenic mouse lines for cartilage-specific inducible overexpression or depletion of *Gata4*
670 to further investigate the role of GATA4 in chondrocytes. Furthermore, studies using GATA4
671 knockdown do not demonstrate a complete reversal of aging in chondrocytes, and additional *in*
672 *vivo* assessment needs to be conducted to verify whether GATA4 could be a therapeutic target for
673 chondrocyte aging. In particular, our *in vitro* study demonstrated the potential of using small-
674 molecule GATA4 to enhance the quality of cartilage created by old chondrocytes. We can validate
675 the findings *in vivo*, as well as develop other GATA4 inhibitors. Lastly, our work indicates that
676 GATA4 has a role in chondrocyte aging, but that does not negate the other aging factors and
677 pathways. Combining current findings and investigating the prevalence of GATA4 in association
678 with other aging molecules will further contribute to our understanding of the role of GATA4 in
679 aging and possible OA onset.
680
681 **Acknowledgments**
682 This work was supported by the Department of Orthopaedic Surgery and the Orland Bethel Family
683 Musculoskeletal Research Center (BMRC) at the University of Pittsburgh, as well as the
684 University of Pittsburgh Center for Research Computing through the resources provided. This
685 study used the Luminex Core Facility of UPCI. M.J.M was supported by the NIH T32 EB001026
686 - Cellular Approaches to Tissue Engineering and Regeneration, Cardiovascular Bioengineering
687 Training Program T32-HL076124, and Ruth L. Kirschstein National Research Service Award
688 (NRSA) Individual Predoctoral Fellowship (Parent F31) 1F31AR083814 - 01A1. The authors
689 thank the funding support from the NIH (P30AG038072). The Chicago Center on Musculoskeletal
690 Pain Research Core Center, supported by NIH P30AR079206, provided training on pain-assessing
691 methods. Schematic figures were created at https://BioRender.com.
692

Data Availability

The Raw and processed RNA-seq data was uploaded to Gene Expression Omnibus (GEO) with accession ID: GSE287861. The data will be publicly available when the manuscript is accepted.

References

1 Xiong, H. *et al.* DNA damage response and GATA4 signaling in cellular senescence and aging-related pathology. *Front Aging Neurosci* **14**, 933015 (2022). https://doi.org:10.3389/fnagi.2022.933015

2 Rahmati, M., Nalesso, G., Mobasheri, A. & Mozafari, M. Aging and osteoarthritis: Central role of the extracellular matrix. *Ageing Res Rev* **40**, 20-30 (2017). https://doi.org:10.1016/j.arr.2017.07.004

3 Makarczyk, M. J. *et al.* Current Models for Development of Disease-Modifying Osteoarthritis Drugs. *Tissue Eng Part C Methods* **27**, 124-138 (2021). https://doi.org:10.1089/ten.TEC.2020.0309

4 Hawker, G. A. & King, L. K. The Burden of Osteoarthritis in Older Adults. *Clin Geriatr Med* **38**, 181-192 (2022). https://doi.org:10.1016/j.cger.2021.11.005

5 Copp, M. E. *et al.* Comet assay for quantification of the increased DNA damage burden in primary human chondrocytes with aging and osteoarthritis. *Aging Cell* **21**, e13698 (2022). https://doi.org:10.1111/acel.13698

6 Loeser, R. F., Collins, J. A. & Diekman, B. O. Ageing and the pathogenesis of osteoarthritis. *Nat Rev Rheumatol* **12**, 412-420 (2016). https://doi.org:10.1038/nrrheum.2016.65

7 Ji, M. L. *et al.* Sirt6 attenuates chondrocyte senescence and osteoarthritis progression. *Nat Commun* **13**, 7658 (2022). https://doi.org:10.1038/s41467-022-35424-w

8 Franceschi, C. *et al.* Inflamm-aging. An evolutionary perspective on immunosenescence. *Ann N Y Acad Sci* **908**, 244-254 (2000). https://doi.org:10.1111/j.1749-6632.2000.tb06651.x

9 Makarczyk, M. J. Cell Therapy Approaches for Articular Cartilage Regeneration. *Organogenesis* **19**, 2278235 (2023). https://doi.org:10.1080/15476278.2023.2278235

10 Shen, J., Li, S. & Chen, D. TGF-beta signaling and the development of osteoarthritis. *Bone Res* **2**, 14002- (2014). https://doi.org:10.1038/boneres.2014.2

11 Roman-Blas, J. A., Stokes, D. G. & Jimenez, S. A. Modulation of TGF-beta signaling by proinflammatory cytokines in articular chondrocytes. *Osteoarthritis Cartilage* **15**, 1367-1377 (2007). https://doi.org:10.1016/j.joca.2007.04.011

12 van der Kraan, P. M. The changing role of TGFbeta in healthy, ageing and osteoarthritic joints. *Nat Rev Rheumatol* **13**, 155-163 (2017). https://doi.org:10.1038/nrrheum.2016.219

13 Kang, C. *et al.* The DNA damage response induces inflammation and senescence by inhibiting autophagy of GATA4. *Science* **349**, aaa5612 (2015). https://doi.org:10.1126/science.aaa5612

14 Qiao, W. *et al.* Lipopolysaccharide-induced DNA damage response activates nuclear factor kappaB signalling pathway via GATA4 in dental pulp cells. *Int Endod J* **52**, 1704-1715 (2019). https://doi.org:10.1111/iej.13180

15 Jia, W. *et al.* GATA4 regulates angiogenesis and persistence of inflammation in rheumatoid arthritis. *Cell Death Dis* **9**, 503 (2018). https://doi.org:10.1038/s41419-018-0570-5

16 Rahman, S. M. T. *et al.* Double knockin mice show NF-kappaB trajectories in immune signaling and aging. *Cell Rep* **41**, 111682 (2022). https://doi.org:10.1016/j.celrep.2022.111682

17 Kang, D. *et al.* Stress-activated miR-204 governs senescent phenotypes of chondrocytes to promote osteoarthritis development. *Sci Transl Med* **11** (2019). https://doi.org:10.1126/scitranslmed.aar6659

18 Schlett, J. S. *et al.* NF-kappaB is a critical mediator of post-mitotic senescence in oligodendrocytes and subsequent white matter loss. *Mol Neurodegener* **18**, 24 (2023). https://doi.org:10.1186/s13024-023-00616-5

19 Li, Z. *et al.* Human Mesenchymal Stem Cell-Derived Miniature Joint System for Disease Modeling and Drug Testing. *Adv Sci (Weinh)* **9**, e2105909 (2022). https://doi.org:10.1002/advs.202105909

20 Glasson, S. S., Blanchet, T. J. & Morris, E. A. The surgical destabilization of the medial meniscus (DMM) model of osteoarthritis in the 129/SvEv mouse. *Osteoarthritis Cartilage* **15**, 1061-1069 (2007). https://doi.org:10.1016/j.joca.2007.03.006

21 Chen, D. *et al.* Osteoarthritis: toward a comprehensive understanding of pathological mechanism. *Bone Res* **5**, 16044 (2017). https://doi.org:10.1038/boneres.2016.44

22 Barton, N. J. *et al.* Pressure application measurement (PAM): a novel behavioural technique for measuring hypersensitivity in a rat model of joint pain. *J Neurosci Methods* **163**, 67-75 (2007). https://doi.org:10.1016/j.jneumeth.2007.02.012

23 Leuchtweis, J., Imhof, A. K., Montechiaro, F., Schaible, H. G. & Boettger, M. K. Validation of the digital pressure application measurement (PAM) device for detection of primary mechanical hyperalgesia in rat and mouse antigen-induced knee joint arthritis. *Methods Find Exp Clin Pharmacol* **32**, 575-583 (2010). https://doi.org:10.1358/mf.2010.32.8.1532102

24 Hayer, S. *et al.* 'SMASH' recommendations for standardised microscopic arthritis scoring of histological sections from inflammatory arthritis animal models. *Ann Rheum Dis* **80**, 714-726 (2021). https://doi.org:10.1136/annrheumdis-2020-219247

25 Wang, X. H. *et al.* GATA4 promotes the senescence of nucleus pulposus cells via NF-kappaB pathway. *Arch Gerontol Geriatr* **101**, 104676 (2022). https://doi.org:10.1016/j.archger.2022.104676

26 Shi, W. *et al.* METTL3 Promotes Activation and Inflammation of FLSs Through the NF-kappaB Signaling Pathway in Rheumatoid Arthritis. *Front Med (Lausanne)* **8**, 607585 (2021). https://doi.org:10.3389/fmed.2021.607585

27 Chen, X. *et al.* METTL3-mediated m(6)A modification of ATG7 regulates autophagy-GATA4 axis to promote cellular senescence and osteoarthritis progression. *Ann Rheum Dis* **81**, 87-99 (2022). https://doi.org:10.1136/annrheumdis-2021-221091

28 Garcia de Vinuesa, A. *et al.* Cripto favors chondrocyte hypertrophy via TGF-beta SMAD1/5 signaling during development of osteoarthritis. *J Pathol* **255**, 330-342 (2021). https://doi.org:10.1002/path.5774

29 Barbero, A. *et al.* Age related changes in human articular chondrocyte yield, proliferation and post-expansion chondrogenic capacity. *Osteoarthritis Cartilage* **12**, 476-484 (2004). https://doi.org:10.1016/j.joca.2004.02.010

30 Forsyth, C. B. *et al.* Increased matrix metalloproteinase-13 production with aging by human articular chondrocytes in response to catabolic stimuli. *J Gerontol A Biol Sci Med Sci* **60**, 1118-1124 (2005). https://doi.org:10.1093/gerona/60.9.1118

31 Shen, H. *et al.* Enhancing the potential of aged human articular chondrocytes for high-quality cartilage regeneration. *FASEB J* **35**, e21410 (2021). https://doi.org:10.1096/fj.202002386R

32 Yeo, E. J. Hypoxia and aging. *Exp Mol Med* **51**, 1-15 (2019). https://doi.org:10.1038/s12276-019-0233-3

33 Hu, S. *et al.* Stabilization of HIF-1alpha alleviates osteoarthritis via enhancing mitophagy. *Cell Death Dis* **11**, 481 (2020). https://doi.org:10.1038/s41419-020-2680-0

34 Zeng, C. Y., Wang, X. F. & Hua, F. Z. HIF-1alpha in Osteoarthritis: From Pathogenesis to Therapeutic Implications. *Front Pharmacol* **13**, 927126 (2022). https://doi.org:10.3389/fphar.2022.927126

35 Romano, O. & Miccio, A. GATA factor transcriptional activity: Insights from genome-wide binding profiles. *IUBMB Life* **72**, 10-26 (2020). https://doi.org:10.1002/iub.2169

36 Dobrzycki, T., Lalwani, M., Telfer, C., Monteiro, R. & Patient, R. The roles and controls of GATA factors in blood and cardiac development. *IUBMB Life* **72**, 39-44 (2020). https://doi.org:10.1002/iub.2178

37 Ang, Y. S. *et al.* Disease Model of GATA4 Mutation Reveals Transcription Factor Cooperativity in Human Cardiogenesis. *Cell* **167**, 1734-1749 e1722 (2016). https://doi.org:10.1016/j.cell.2016.11.033

38 Villamayor, L., Cano, D. A. & Rojas, A. GATA factors in pancreas development and disease. *IUBMB Life* **72**, 80-88 (2020). https://doi.org:10.1002/iub.2170

39 Tremblay, M., Sanchez-Ferras, O. & Bouchard, M. GATA transcription factors in development and disease. *Development* **145** (2018). https://doi.org:10.1242/dev.164384

40 Molkentin, J. D. The zinc finger-containing transcription factors GATA-4, -5, and -6. Ubiquitously expressed regulators of tissue-specific gene expression. *J Biol Chem* **275**, 38949-38952 (2000). https://doi.org:10.1074/jbc.R000029200

41 Jiao, H., Walczak, B. E., Lee, M. S., Lemieux, M. E. & Li, W. J. GATA6 regulates aging of human mesenchymal stem/stromal cells. *Stem Cells* **39**, 62-77 (2021). https://doi.org:10.1002/stem.3297

42 Mahmoud, M., Souilhol, C., Serbanovic-Canic, J. & Evans, P. GATA4-Twist1 Signalling in Disturbed Flow-Induced Atherosclerosis. *Cardiovasc Drugs Ther* **33**, 231-237 (2019). https://doi.org:10.1007/s10557-019-06863-3

43 Katanasaka, Y., Suzuki, H., Sunagawa, Y., Hasegawa, K. & Morimoto, T. Regulation of Cardiac Transcription Factor GATA4 by Post-Translational Modification in Cardiomyocyte Hypertrophy and Heart Failure. *Int Heart J* **57**, 672-675 (2016). https://doi.org:10.1536/ihj.16-404

44 Patankar, J. V. *et al.* Loss of intestinal GATA4 prevents diet-induced obesity and promotes insulin sensitivity in mice. *Am J Physiol Endocrinol Metab* **300**, E478-488 (2011). https://doi.org:10.1152/ajpendo.00457.2010

45 Patankar, J. V. *et al.* Intestinal GATA4 deficiency protects from diet-induced hepatic steatosis. *J Hepatol* **57**, 1061-1068 (2012). https://doi.org:10.1016/j.jhep.2012.06.028

46 Meurot, C. *et al.* Targeting the GLP-1/GLP-1R axis to treat osteoarthritis: A new opportunity? *J Orthop Translat* **32**, 121-129 (2022). https://doi.org:10.1016/j.jot.2022.02.001

47 Yang, Y. *et al.* Osteoarthritis treatment via the GLP-1-mediated gut-joint axis targets intestinal FXR signaling. *Science* **388**, eadt0548 (2025). https://doi.org:10.1126/science.adt0548

48 Chung, Y. P., Weng, T. I., Chan, D. C., Yang, R. S. & Liu, S. H. Low-dose tributyltin triggers human chondrocyte senescence and mouse articular cartilage aging. *Arch Toxicol* **97**, 547-559 (2023). https://doi.org:10.1007/s00204-022-03407-x

49 Chung, Y. P., Chen, Y. W., Weng, T. I., Yang, R. S. & Liu, S. H. Arsenic induces human chondrocyte senescence and accelerates rat articular cartilage aging. *Arch Toxicol* **94**, 89-101 (2020). https://doi.org:10.1007/s00204-019-02607-2

50 Thielen, N. G. M. *et al.* Separating friend from foe: Inhibition of TGF-beta-induced detrimental SMAD1/5/9 phosphorylation while maintaining protective SMAD2/3 signaling in OA chondrocytes. *Osteoarthritis Cartilage* **31**, 1481-1490 (2023). https://doi.org:10.1016/j.joca.2023.08.004

51 van der Kraan, P. M., Goumans, M. J., Blaney Davidson, E. & ten Dijke, P. Age-dependent alteration of TGF-beta signalling in osteoarthritis. *Cell Tissue Res* **347**, 257-265 (2012). https://doi.org:10.1007/s00441-011-1194-6

52 Bauge, C., Girard, N., Lhuissier, E., Bazille, C. & Boumediene, K. Regulation and Role of TGFbeta Signaling Pathway in Aging and Osteoarthritis Joints. *Aging Dis* **5**, 394-405 (2014). https://doi.org:10.14336/AD.2014.0500394

53 van Caam, A. *et al.* TGFbeta1-induced SMAD2/3 and SMAD1/5 phosphorylation are both ALK5-kinase-dependent in primary chondrocytes and mediated by TAK1 kinase activity. *Arthritis Res Ther* **19**, 112 (2017). https://doi.org:10.1186/s13075-017-1302-4

54 Wiegertjes, R. *et al.* Increased IL-6 receptor expression and signaling in ageing cartilage can be explained by loss of TGF-beta-mediated IL-6 receptor suppression. *Osteoarthritis Cartilage* **29**, 773-782 (2021). https://doi.org:10.1016/j.joca.2021.01.008

55 Lee, G. T. *et al.* Induction of interleukin-6 expression by bone morphogenetic protein-6 in macrophages requires both SMAD and p38 signaling pathways. *J Biol Chem* **285**, 39401-39408 (2010). https://doi.org:10.1074/jbc.M110.103705

56 Guemes, M. *et al.* GATA4 is essential for bone mineralization via ERalpha and TGFbeta/BMP pathways. *J Bone Miner Res* **29**, 2676-2687 (2014). https://doi.org:10.1002/jbmr.2296

57 Iijima, H. *et al.* Age-related matrix stiffening epigenetically regulates alpha-Klotho expression and compromises chondrocyte integrity. *Nat Commun* **14**, 18 (2023). https://doi.org:10.1038/s41467-022-35359-2

58 Grogan, S. P. & D'Lima, D. D. Joint aging and chondrocyte cell death. *Int J Clin Rheumtol* **5**, 199-214 (2010). https://doi.org:10.2217/ijr.10.3

59 Fu, B. *et al.* Matrix stiffening promotes chondrocyte senescence and the osteoarthritis development through downregulating HDAC3. *Bone Res* **12**, 32 (2024). https://doi.org:10.1038/s41413-024-00333-9

60 Vincent, T. L. Targeting mechanotransduction pathways in osteoarthritis: a focus on the pericellular matrix. *Curr Opin Pharmacol* **13**, 449-454 (2013). https://doi.org:10.1016/j.coph.2013.01.010

61 Massague, J. TGFbeta signalling in context. *Nat Rev Mol Cell Biol* **13**, 616-630 (2012). https://doi.org:10.1038/nrm3434

62 Allen, J. L., Cooke, M. E. & Alliston, T. ECM stiffness primes the TGFbeta pathway to promote chondrocyte differentiation. *Mol Biol Cell* **23**, 3731-3742 (2012). https://doi.org:10.1091/mbc.E12-03-0172

63 Chery, D. R. *et al.* Decorin regulates cartilage pericellular matrix micromechanobiology. *Matrix Biol* **96**, 1-17 (2021). https://doi.org:10.1016/j.matbio.2020.11.002

64 Li, Q. *et al.* Mediation of Cartilage Matrix Degeneration and Fibrillation by Decorin in Post-traumatic Osteoarthritis. *Arthritis Rheumatol* **72**, 1266-1277 (2020). https://doi.org:10.1002/art.41254

65 Chu, W. C. *et al.* Distribution of pericellular matrix molecules in the temporomandibular joint and their chondroprotective effects against inflammation. *Int J Oral Sci* **9**, 43-52 (2017). https://doi.org:10.1038/ijos.2016.57

66 Yao, Q. *et al.* Osteoarthritis: pathogenic signaling pathways and therapeutic targets. *Signal Transduct Target Ther* **8**, 56 (2023). https://doi.org:10.1038/s41392-023-01330-w

67 Adler, A. S. *et al.* Motif module map reveals enforcement of aging by continual NF-kappaB activity. *Genes Dev* **21**, 3244-3257 (2007). https://doi.org:10.1101/gad.1588507

68 Marechal, A. & Zou, L. DNA damage sensing by the ATM and ATR kinases. *Cold Spring Harb Perspect Biol* **5** (2013). https://doi.org:10.1101/cshperspect.a012716

69 Menolfi, D. & Zha, S. ATM, ATR and DNA-PKcs kinases-the lessons from the mouse models: inhibition not equal deletion. *Cell Biosci* **10**, 8 (2020). https://doi.org:10.1186/s13578-020-0376-x

70 Wang, Y. *et al.* Autophagy Regulates Chromatin Ubiquitination in DNA Damage Response through Elimination of SQSTM1/p62. *Mol Cell* **63**, 34-48 (2016). https://doi.org:10.1016/j.molcel.2016.05.027

71 Yousefzadeh, M. *et al.* DNA damage-how and why we age? *Elife* **10** (2021). https://doi.org:10.7554/eLife.62852

72 Sarkar, A. *et al.* STAT3 promotes a youthful epigenetic state in articular chondrocytes. *Aging Cell* **22**, e13773 (2023). https://doi.org:10.1111/acel.13773

Supplementary Figures and Tables

Figure S1

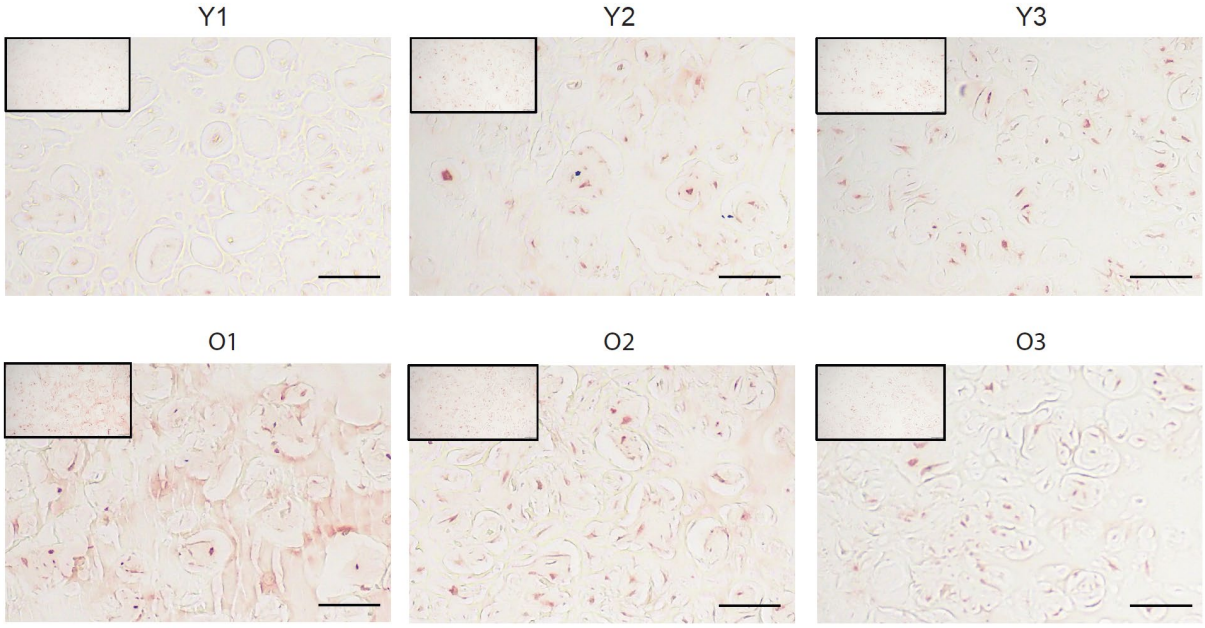

Figure S1. *GATA4 IHC of healthy human cartilage tissue from 3 young (Y1,Y2, Y3) and aged (O1,O2, O3) donors. Scale Bar=50 µm.*

Figure S2

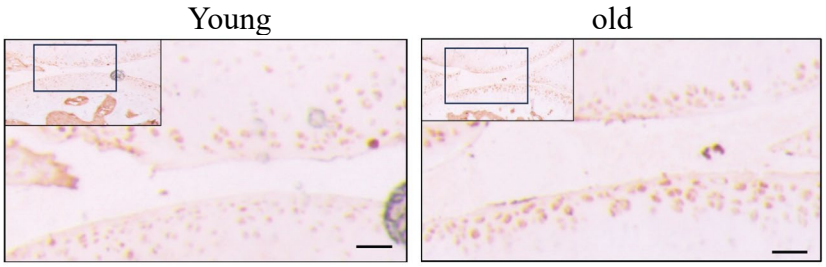

Figure S2. *GATA4 IHC of healthy mouse cartilage tissue from young (left) and old (right) mice. Scale Bar=50 µm.*

Figure S3

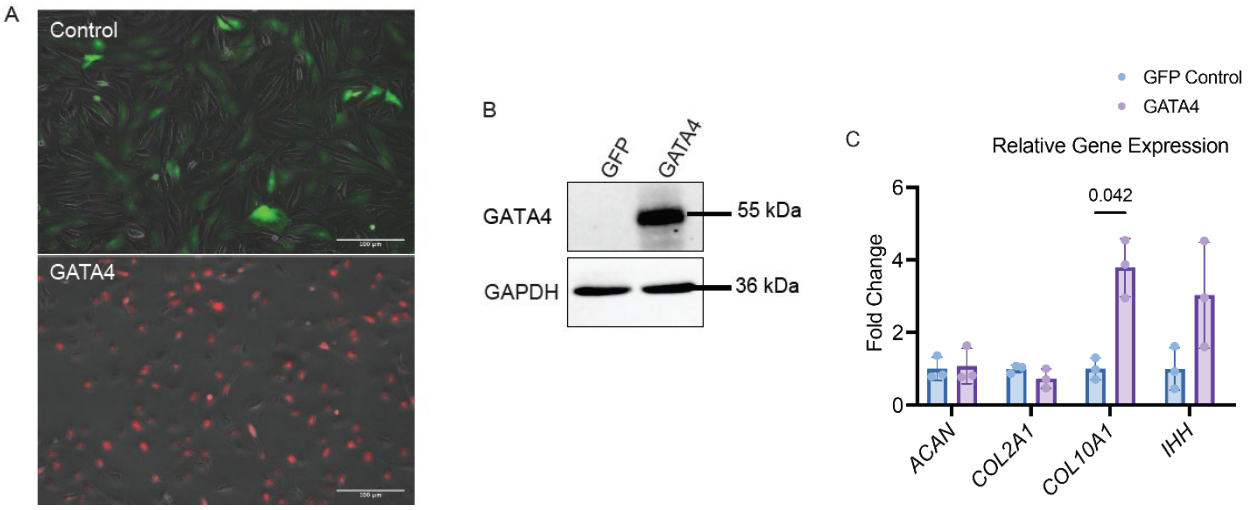

Figure S3. *(A) GATA4 overexpression of young, pooled chondrocytes in monolayer culture 48 hours after infection. The lentiviral control contained the EF1A promoter-driven expression of Green Fluorescent Protein (GFP), and the GATA4 lentivirus contained the EF1A promoter-driven overexpression of GATA4 with dTomato fluorescent protein. Scale Bar=100 µm. (B) Western blot to measure GATA4 protein levels. (C) RT-qPCR analysis of relative gene expression of cartilage matrix proteins aggrecan (ACAN) and collagen type II-α1 (COL2A1), and hypertrophy markers collagen type X- α1 (COL10A1) and India hedgehog (IHH).*

963 **Figure S4**

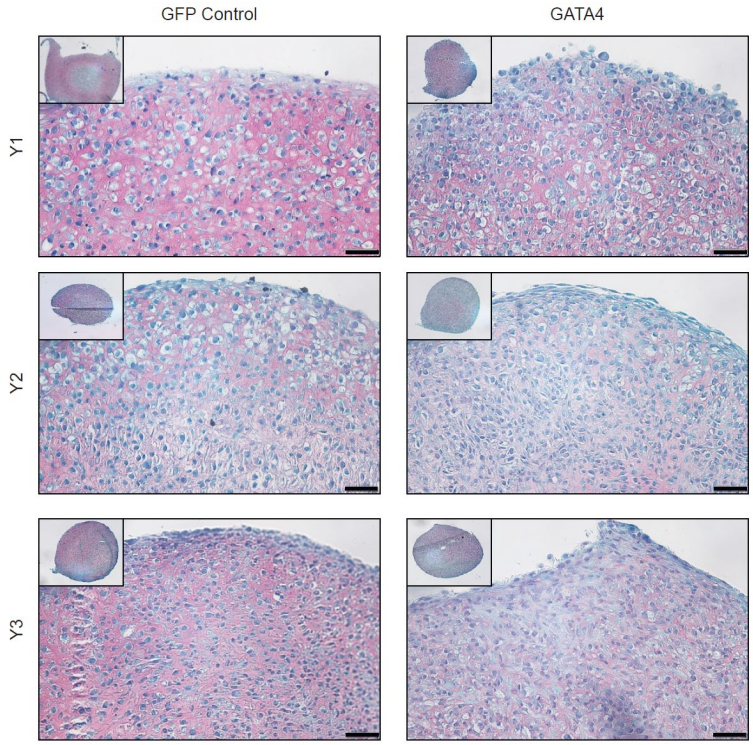

964

965 ***Figure S4.*** *Safranin-O staining for pellets derived from young, individual chondrocyte (Y1-3)*
966 *transduced with GFP control lentivirus or GATA4 lentivirus. Pellets were cultured in chondrogenic*
967 *medium for 7 days. Scale Bar=50 μm.*
968
969
970
971
972
973 ***Figure S5***
974

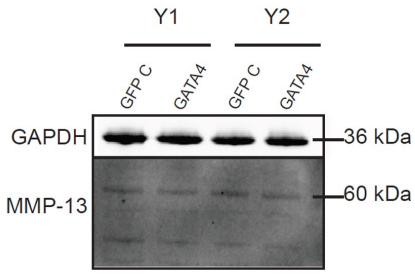

975
976
977 ***Figure S5.*** *Western blot to examine MMP-13 protein levels in pellets derived from two young*
978 *chondrocyte lines (Y1 and Y2) overexpressing GFP control (GFP C) or GATA4.*
979
980
981
982

983 ***Figure S6***

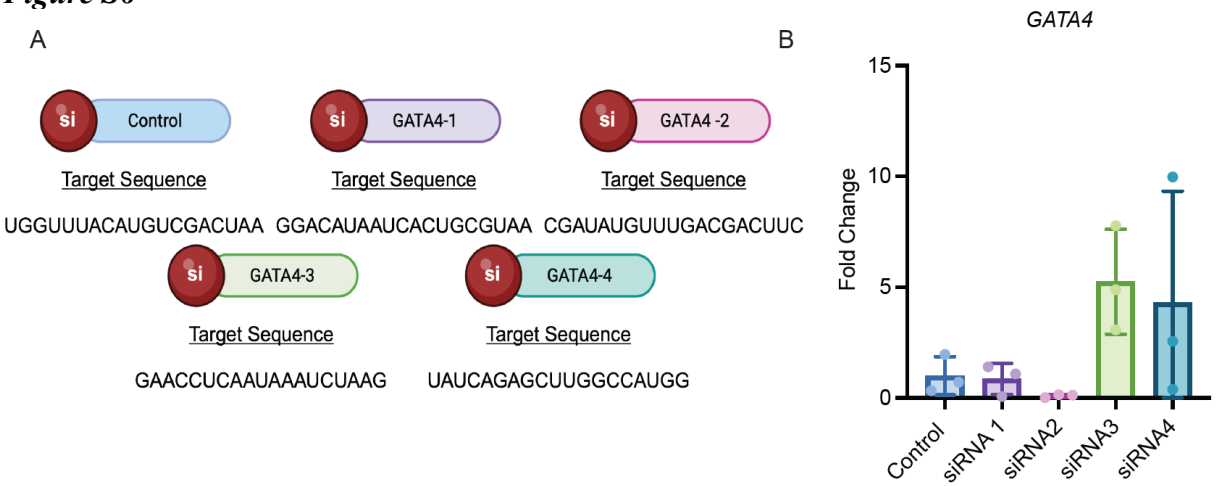

984
985 ***Supplementary Figure 6. Assessment of GATA4 siRNAs in monolayer***. *(A) Schematic of the four*
986 *different GATA4 siRNAs with corresponding target sequences assessed for GATA4 knockdown in*
987 *monolayer culture of old pooled chondrocytes. (B) RT-qPCR assessing GATA4 levels after siRNA*
988 *treatment (n=3). Created in BioRender. Makarczyk, M. (2025) https://BioRender.com/luon9t1*
989
990
991
992 **Figure S7**

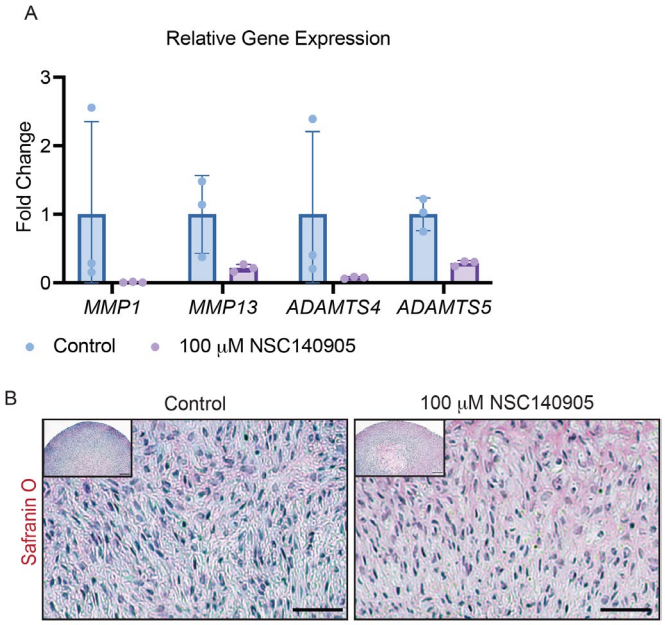

993
994 ***Supplementary Figure 7. Assessment of GATA4 small molecule inhibitor, NSC140905.*** *Pooled*
995 *old human chondrocytes were pelleted and treated with the chondrogenic medium with or without*
996 *supplanting NSC140905 for 14 days. (A) RT-qPCR analysis of relative gene expression of matrix-*
997 *degrading enzymes, including MMP-1,13 and ADAMTS 4 and 5 (n=3). Student's two-tailed t-test*
998 *with Welch's correction for standard deviation and a p-value of 0.05 was used for all statistical*
999 *analysis. (B) Safranin-O/Fast green staining. Bar=50 μM.*
1000

1001 **Figure S8**

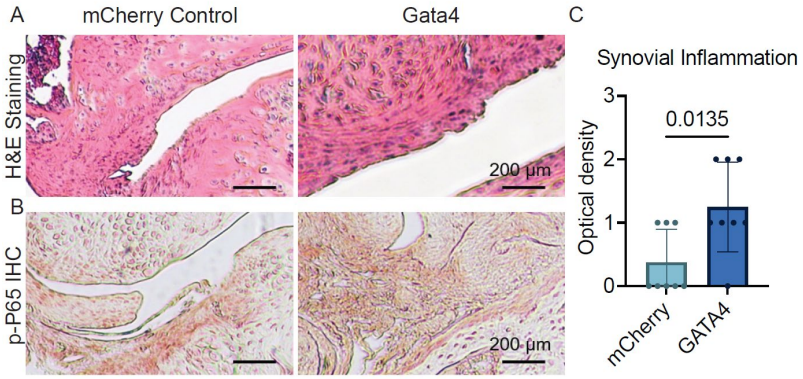

1002
1003 ***Supplementary Figure S8.*** *(A) H&E staining and (B) p-P65 IHC to assess synovial inflammation*
1004 *in mice treated with lentiviral vectors carrying mCherry Control or Gata4.* C. p-P65 IHC staining
1005 was also semi-quantitated.
1006
1007
1008
1009
1010
1011 **Figure S9**

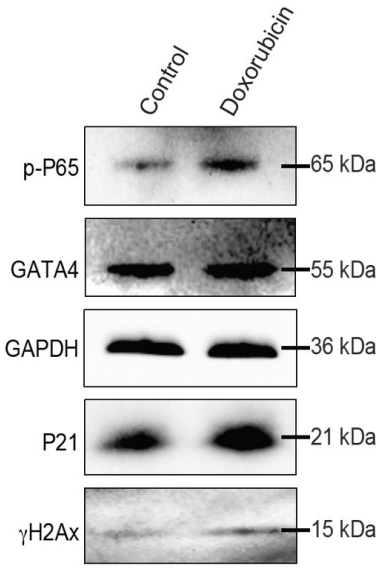

1012
1013 ***Supplementary Figure S9.*** *Wester blot to examine protein levels in chondrocytes treated with*
1014 *doxorubicin (100nM) or vehicle control for 3 days.*
1015
1016
1017
1018
1019
1020
1021
1022

1023 **Table S1. Information of chondrocyte donors**

1024 RNA sequencing

Age	Gender
24	Female
36	Female
38	Female
70	Female
73	Female
74	Female

1025

1026 Western Blot

Age	Gender
22	Male
26	Male
29	Male
69	Male
70	Male
73	Female

1027

1028

1029 Human Cartilage Tissue IHC

Age	Gender
24	Male
25	Female
27	Female
33	Male
67	Female
76	Female
78-1	Female
78-2	Male

1030

1031 Young Chondrocyte Pool

Age	Gender
22	Male
29	Male
38	Female
42	Female

1032

1033 Old Chondrocyte Pool #1

Age	Gender
66	Male
70	Male
73	Female

1034

1035 Old Chondrocyte Pool #2

Age	Gender
66-1	Male
66-2	Male
70-1	Male
70-2	Male

Monolayer young individual chondrocytes

Age	Gender
29	Male
36	Female
38	Female

Pellet young individual chondrocytes

Age	Gender
21	Male
35	Male
38	Female

1042 **Table S2. Antibodies used for immunofluorescence (IF), Immunohistochemistry (IHC), or**
1043 **Western blot (WB)**

Antibody	Origin	Cat. No	Species	Assay	Dilution
Anti-Human Collagen Type II	MP Biomedicals	SKU 0863171	Mouse	IHC	1:200
Biotinylated Goat Anti-Rabbit IgG	Vector Laboratories	PK-6101	Rabbit	IHC	1:50
Goat Anti-Rabbit IgG H&L (HRP)	Abcam	Ab6721	Goat	WB	1:5000
GAPDH (D16H11) XP® Rabbit mAb	Cell Signaling Technology	5174s	Rabbit	WB	1:2000
Smad1 (D59D7) XP® Rabbit mAb	Cell Signaling Technology	6944s	Rabbit	WB	1:500
Anti-GATA4 antibody (ab84593)- Discontinued	Abcam	ab84593	Rabbit	IHC/WB	1:500
GATA-4 (D3A3M) Rabbit mAb	Cell Signaling Technology	369366s	Rabbit	IHC/WB	1:1000
Phospho-Smad1/5 (Ser463/465) (41D10) Rabbit mAb	Cell Signaling Technology	9516s	Rabbit	WB	1:500
Phospho-Smad2 (Ser465/467) (138D4) Rabbit mAb	Cell Signaling Technology	3108s	Rabbit	WB	1:500
Smad2/3 (D7G7) XP® Rabbit mAb	Cell Signaling Technology	8685s	Rabbit	WB	1:500
Anti-NF-kB p65 (phospho S536) antibody [EP2294Y]	Abcam	ab76302	Rabbit	WB	1:500
Anti-NF-kB p65 antibody [E379]	Abcam	ab32536	Rabbit	WB	1:500
Anti-p21 antibody [EPR362] - BSA and Azide free	Abcam	ab218311	Rabbit	WB	1:1000
Phospho-Histone H2A.X (Ser139) (20E3) Rabbit mAb	Cell Signaling Technology	9718s	Rabbit	WB	1:500

1044
1045
1046
1047
1048
1049

1050 **Table S3: Full names of genes shown in Figure 1**

Transcription Regulator Name	Acronym
Hypoxia-inducible factor 1-alpha	HIF1A
GATA binding protein 4	GATA4
MAF bZIP transcription factor B	MAFB
Homeobox D10	HOXD10
CCAAT enhancer binding protein alpha	CEBPA
Forkhead box L2	FOXL2
Caudal type homeobox 2	CDX2
Early Growth Response 1	EGR1
Signal Transducer and Activator of Transcription 3	STAT3
Paired Box 1	PAX1
Sequestosome 1	SQSTM1
Myocardin Related Transcription Factor B	MRTFB
WW Domain Binding Protein 2	WBP2
Scleraxis bHLH Transcription Factor	SCX
Twist Family bHLH Transcription Factor 1	TWIST1
Myocyte Enhancer Factor 2D	MEF2D
Lysine Methyltransferase 2D	KMT2D
Achaete-scute Family bHLH Transcription Factor 1	ASCL1
Recombination Signal Binding Protein for Immunoglobulin kappa J region	RBPJ
SIX homeobox 1	SIX1
FERM domain containing 3	FRMPD3
Ceruloplasmin	CP
SPARC related modular calcium binding 2	SMOC2
ATP binding cassette subfamily A member 13	ABCA13
Inositol 1,4,5-triphosphate receptor type 1	ITPR1
NIM1 serine/threonine protein kinase	NIM1K
Fibroblast growth factor 13	FGF13
Ankyrin repeat domain 12	ANKRD12
GTP binding protein overexpressed in skeletal muscle	GEM
erythroferrone	FAM132B
Pappalysin 1	PAPPA
PPARG coactivator 1 alpha	PPARGC1A
Synaptotagmin like 2	SYTL2
Leucine rich repeat transmembrane neuronal 2	LRRTM2
G protein-coupled receptor class C group 5 member B	GPRC5B
Polypeptide N-acetylgalactosaminyltransferase 15	GALNT15

Growth associated protein 43	GAP43
Fibroblast growth factor binding protein 1	FGFBP1
ATRX chromatin remodeler	ATRX
Protocadherin gamma subfamily B, 2	PCDHGB2
Calsyntenin 2	CLSTN2
Fibroblast growth factor binding protein 2	FGFBP2
Desmocollin 2	DSC2
TNF receptor superfamily member 21	TNFRSF21
Kinesin family member 13B	KIF13B
Plexin A2	PLXNA2
Cysteine rich protein 2	CRIP2
Cysteine rich protein 1	CRIP1
KLF transcription factor 2	KLF2
Serum/glucocorticoid regulated kinase 1	SGK1
LIM zinc finger domain containing 2	LIMS2
Long intergenic non-protein coding RNA 1133	LINC01133
Adipogenesis regulatory factor	ADIRF
Ornithine decarboxylase 1	ODC1
Kazrin, periplakin interacting protein	KAZN
Chondroitin polymerizing factor	CHPF
RAB23, member RAS oncogene family	RAB23
Alkaline phosphatase, biomineralization associated	ALPL
Signal transducer and activator of transcription 4	STAT4
G protein-coupled receptor 1	GPR1
Spectrin alpha, non-erythrocytic 1	SPTAN1
Very low density lipoprotein receptor	VLDLR
Fatty acid desaturase 3	FADS3
Cancer susceptibility candidate 4	CASC4
NAD(P)H quinone dehydrogenase 1	NQO1
Pyrroline-5-carboxylate reductase 1	PYCR1
ERBB receptor feedback inhibitor 1	ERRFI1
NmrA-like family domain containing 1 pseudogene	LOC344887
Desumoylating isopeptidase 2	DESI2
Basonuclin zinc finger protein 1	BNC1

1051

1052

1053 **Table S4. Primers for qRT-PCR**

Gene	Forward primer (5'-3')	Reverse primer (5'-3')
RPL13A	GCCATCGTGGCTAAACAGGTA	GTTGGTGTTCATCCGCTTGC
GATA4	CAGTCTACGTGCCCACACC	TCCCGCCTGGCTCCAT
ACAN	AGTCACACCTGAGCAGCATC	AGTTCTCAAATTGCATGGGGTGTC
COL2A1	GGATGGCTGCACGAAACATACCGG	CAAGAAGCAGACCGGCCCTATG
COL10A1	CCCTCTTGTTAGTGCCAACC	AGATTCCAGTCCTTGGGTCA
IHH	AACTCGCTGGCTATCTCGGT	GCCCTCATAATGCAGGGACT
IL-6	ACTCACCTCTTCAGAACGAATTG	CCATCTTTGGAAGGTTCAGGTTG
IL-8	TTTTGCCAAGGAGTGCTAAAGA	AACCCTCTGCACCCAGTTTTC
TNF-α	CCTCTCTCTAATCAGCCCTCTG	GAGGACCTGGGAGTAGATGAG
MMP-1	AAAATTACACGCCAGATTTGCC	GGTGTGACATTACTCCAGAGTTG
MMP-2	GGTCACATCGCTCCAGACT	TACAGGATCATTGGCTACACACC
MMP-3	CGGTTCCGCCTGTCTCAAG	CGCCAAAAGTGCCTGTCTT
MMP-12	GGAATCCTAGCCCATGCTTTT	CATTACGGCCTTTGGATCACT
MMP-13	ACTGAGAGGCTCCGAGAAATG	GAACCCCGCATCTTGGCTT
ADAMTS4	GAGGAGGAGATCGTGTTTCCA	CCAGCTCTAGTAGCAGCGTC
ADAMTS5	GAACATCGACCAACTCTACTCCG	CAATGCCCACCGAACCATCT

1054

1055

1056

1057 **Table S5. Information of Luminex assay kit**

Target Molecule	Method	Catalog number & supplier
IL-8	Luminex® assay	HAGP1MAG-12K, EMD Millipore
IL-6, CCL2, MMP-1, MMP-2, MMP-13.	Luminex® assay	LXSAHM-18, R&D Systems

1058

1059 **Supplementary Table 6: Comprehensive list of proteins assessed in LUMINEX**

Target Molecule	Catalog number & supplier
Interleukin-6 (IL-6)	LXSAHM-18, R&D Systems
Interleukin-13 (IL-13)	LXSAHM-18, R&D Systems
Matrix Metallopeptidase-3 (MMP-3)	LXSAHM-18, R&D Systems

Periostin (OSF-2)	LXSAHM-18, R&D Systems
Vascular Endothelial Growth Factor Receptor 2 (VEGFR2)	LXSAHM-18, R&D Systems
MMP-8	LXSAHM-18, R&D Systems
Adiponectin (AdipoQ)	LXSAHM-18, R&D Systems
Complement Factor D/Adipsin (CFD)	LXSAHM-18, R&D Systems
Ectonucleotide Pyrophosphatase/Phosphodiesterase 2 Autotaxin (ENPP-2)	LXSAHM-18, R&D Systems
MMP-2	LXSAHM-18, R&D Systems
Osteopontin (OPN)	LXSAHM-18, R&D Systems
C-C motif ligand 2 (CCL2)	LXSAHM-18, R&D Systems
(C-X-C motif) ligand 1 (CXCL1)	LXSAHM-18, R&D Systems
IL-1ra	LXSAHM-18, R&D Systems
MMP-1	LXSAHM-18, R&D Systems
MMP-13	LXSAHM-18, R&D Systems
Tissue Inhibitor of Metalloproteinase-1 (TIMP-1)	HTMP1MAG-54K, EMD Millipore
TIMP-2	HTMP1MAG-54K, EMD Millipore
Angiopoietin-2 (Ang-2)	HAGP1MAG-12K, EMD Millipore
Bone Morphogenic Protein-9 (BMP-9)	HAGP1MAG-12K, EMD Millipore
Epidermal Growth Factor (EGF)	HAGP1MAG-12K, EMD Millipore
Endoglin (CD105)	HAGP1MAG-12K, EMD Millipore
Endothelin-1 (ET-1)	HAGP1MAG-12K, EMD Millipore
Fibroblast Growth Factor-1 (FGF-1)	HAGP1MAG-12K, EMD Millipore
FGF-2	HAGP1MAG-12K, EMD Millipore
Follistatin (FSH)	HAGP1MAG-12K, EMD Millipore
Granulocyte Colony Stimulating Factor (G-CSF)	HAGP1MAG-12K, EMD Millipore
Heparin-Binding EGF-like Growth Factor HB-EGF	HAGP1MAG-12K, EMD Millipore
Hepatocyte Growth Factor (HGF)	HAGP1MAG-12K, EMD Millipore
IL-8	HAGP1MAG-12K, EMD Millipore

Leptin (LEP)	HAGP1MAG-12K, EMD Millipore
Placental Growth Factor (PLGF)	HAGP1MAG-12K, EMD Millipore
VEGF-A	HAGP1MAG-12K, EMD Millipore
VEGF-D	HAGP1MAG-12K, EMD Millipore